

DETECTION OF COSMIC DARK MATTER

Joel R. Primack and David Seckel

Santa Cruz Institute for Particle Physics, University of California,
Santa Cruz, California 95064

Bernard Sadoulet

Physics Department, University of California, Berkeley, California 94720

CONTENTS

1. INTRODUCTION	751
1.1 <i>How Much DM Is There?</i>	752
1.2 <i>Arguments That DM Is Nonbaryonic</i>	754
1.3 <i>Nonbaryonic DM Candidates</i>	755
2. WEAKLY INTERACTING MASSIVE PARTICLES.....	756
2.1 <i>Motivation for and Properties of WIMP Candidates</i>	756
2.2 <i>Interaction Rates of WIMPs with Ordinary Matter</i>	762
2.3 <i>Direct Detection by Nuclear Recoil</i>	768
2.4 <i>Indirect Detection by Annihilation</i>	783
2.5 <i>Present Constraints and Future Prospects</i>	791
3. AXIONIC DARK MATTER.....	792
3.1 <i>Motivation</i>	792
3.2 <i>Cosmological and Astrophysical Constraints</i>	793
3.3 <i>Detection by Conversion to Photons in Laboratory Experiments</i>	795
3.4 <i>Theoretical Uncertainties</i>	795
4. LIGHT NEUTRINOS.....	796
5. SUMMARY	798
5.1 <i>Uncertainties</i>	799
5.2 <i>What If?</i>	799

1. INTRODUCTION

There is excellent observational evidence (1-4) that at least 90% of the mass in the universe is invisible; that is, it neither emits nor absorbs electromagnetic radiation of any frequency. The determination of the

nature of this “dark matter” (DM) is one of the most important questions confronting modern physics and astronomy. In this article, we review the prospects for direct detection of nonbaryonic DM candidates through their interactions with detectors in terrestrial laboratories, and for indirect detection via observation of radiation (neutrinos, gamma rays, antiprotons, etc) from DM annihilation in the Earth, Sun, or galactic halo. Smith (5) reviewed earlier work on direct detection.

1.1 How Much DM Is There?

The available information about the average density of matter in the universe is summarized in Table 1. The symbols in the table are as follows: $\Omega \equiv \rho/\rho_c$ is the cosmological density in units of critical density $\rho_c \equiv 3H_0^2/8\pi G = 1.9 \times 10^{-29} h^2 \text{ g cm}^{-3} = 11h^2 \text{ keV cm}^{-3} = 2.8 \times 10^{11} h^2 M_\odot \text{ Mpc}^{-3}$, distances are measured in parsecs (1 pc = 3.09×10^{18} cm = 3.26 light years), and $h \approx 0.5\text{--}1$ is the Hubble parameter H_0 in units of $100 \text{ km s}^{-1} \text{ Mpc}^{-1}$. Ω is the total density, including both luminous matter (stars, gas) and DM. In all but the last two lines of Table 1, Ω is inferred using standard gravitational theory from velocities observed on the scale indicated. References for the information in Table 1 and the following two paragraphs are given in (1–4). A recent attempt to determine Ω from observation of galaxies at fairly high redshift (a “cosmological test”) is discussed below, as are theoretical arguments that $\Omega = 1$.

The strongest evidence for DM comes from studies of the masses of individual galaxies and of groups and clusters of galaxies. The flat or rising optical rotation curves (6) that have been obtained for more than a hundred spiral galaxies are hard [but perhaps not impossible (7)] to understand without $M_{\text{tot}}/M_{\text{vis}}$ rising with radius to about 2–3 at the optical radius. In a few dozen nearby galaxies, the availability of more distant test particles has allowed astronomers to verify that there is more nonluminous mass at larger radii. Radio observations of the Doppler shifts of the disks of

Table 1 Cosmological density estimates

	Scale ($\times h^{-1}$ Mpc)	Ω
Luminous parts of galaxies	~ 0.02	0.01
Halos of galaxies and groups of galaxies	$\sim 0.1\text{--}1$	0.02–0.2
Cosmic virial theorem	~ 3	~ 0.2
Virgo infall	~ 10	~ 0.2
Large-scale infall	~ 30	$\sim 0.2\text{--}1$
Cosmological tests	3000	0.1–2
Cosmic inflation		1

neutral hydrogen around those few spiral galaxies where the 21-cm emission can be detected to 2–3 optical radii require the presence of $M_{\text{tot}}/M_{\text{vis}} \gtrsim 3\text{--}10$ in order to provide the gravitational attraction to bind gas of such high rotational velocity. Mass estimates in the same range come from studies of the dynamics of the stellar, gas cloud, globular cluster, and dwarf galaxy satellites of the Milky Way. Observations of the velocity dispersion of the globular clusters, the rotation velocity of rings of stars or gas, the pattern of “shells” of stars, the distribution of x-ray emitting gas, and the dynamics of the satellites of S0 and elliptical galaxies again give mass estimates in the same range.

The stability of disk galaxies against bar formation, the “flaring” and warps of the atomic hydrogen (HI) gas observed in a few galactic disks at large radii, and the velocity of satellite rings of gas perpendicular to the disk in a few S0 galaxies all suggest that the DM halos of disk galaxies are approximately spherical or spheroidal. The observed flat rotation curves imply that, roughly, $M_{\text{DM}}(< r) \propto r$, or $\rho_{\text{DM}}(r) \propto r^{-2}$. Thus the stars, dust, and gas form a centrally condensed spheroid and/or thin disk, while the DM is spread out over a much larger volume. This suggests that the DM is dissipationless, in contrast to the visible matter, which loses kinetic energy by radiation, sinks to the center of the galaxy, and forms a disk when dissipative infall is halted by angular momentum conservation (8). This picture of spiral galaxy formation by infall within a dissipationless DM halo (9) provides a natural explanation of the origin of the relatively large observed angular momenta of galactic disks (10) as well as the flatness of observed rotation curves (11–15).

As Table 1 summarizes, only $\Omega \lesssim 0.2$ is associated with halos of groups and clusters of galaxies. The amount of DM on larger scales is uncertain, in part because it is not known how this DM is distributed. If the DM is clustered in the same way as the galaxies, then $\Omega \sim 0.2$ (16). But if the DM is less clustered than the galaxies, as occurs in theories of “biased” galaxy formation (17), it is possible that $\Omega_{\text{DM}} \approx 1$.

The Infrared Astronomical Satellite (IRAS) survey has attempted to map the density structure of the universe out to $100h^{-1}$ Mpc. The very preliminary result from this effort, which is the largest-scale galaxy redshift survey that has yet been used to estimate Ω , is $\Omega \approx 0.5$ (18).

It is difficult to distinguish geometrical from evolutionary effects in cosmological measurements that bear on the global value of Ω . Although a recent measurement of galaxy counts as a function of redshift (19) suggests that $\Omega \gtrsim 0.4$, the interpretation of these data is quite uncertain (20).

Theoretical prejudice favors $\Omega = 1$ for at least three reasons:

1. $\Omega = 1$ is the uniquely stable value for Friedmann cosmologies. If Ω

is larger or smaller than unity at early times, it deviates increasingly as time goes on. Since Ω_0 (the subscript 0 denotes the present epoch) is known to be within an order of magnitude of unity, it perhaps seems most plausible that there is nothing special about the present epoch and Ω is exactly unity.

2. The hypothesis of cosmic inflation (21, 22)—that the universe underwent exponential expansion during an early brief phase when the vacuum energy dominated—leads to the prediction of vanishing curvature $k = \Omega - \Omega_\Lambda - 1 = 0$, where $\Omega_\Lambda = \Lambda/3H^2$. Fundamental theory still does not predict the value of the cosmological constant Λ (but see 23, 24). But since the observational upper limit $|\Omega_\Lambda| \lesssim 1$ implies a bound on Λ that is many orders of magnitude smaller than any known particle physics scale, it is frequently supposed that this bound will be easiest to understand if Λ vanishes exactly.

3. If galaxies and clusters arose from density fluctuations in the early universe as is commonly supposed, this implies lower limits on the amplitude of these density fluctuations at the era of recombination, which in turn imply model-dependent lower limits on the magnitude of the fluctuations $\delta T/T$ in the cosmic background radiation (CBR) on the angular scale of a few arcminutes (25–29). Because the fluctuation amplitude grows more slowly with time in a low-density universe, for models such as cold DM these lower limits on $\delta T/T$ are in serious conflict with the latest upper limits on $\delta T/T$ (30, 31) if $\Omega_0 \approx 0.2$, but not (yet) in trouble if $\Omega_0 = 1$.

Despite these powerful arguments, we advocate keeping an open mind about the values of Ω_0 and Λ . However, in this paper we henceforth assume that $\Omega = 1$ and $\Lambda = 0$.

1.2 Arguments That DM Is Nonbaryonic

The agreement (32) between the standard primordial nucleosynthesis calculations and the observed abundances of the light nuclides (H, D, ^3He , ^4He , ^6Li , ^7Li) has generally been regarded as a pillar of the standard hot big bang model and a triumph for theoretical cosmology. But this works well only if the density Ω_b of ordinary (“baryonic”) matter—i.e. atoms and ions—lies in the range $0.014h^{-2} \lesssim \Omega_b \lesssim 0.025h^{-2}$, with a firm upper limit

$$\Omega_b \lesssim 0.035h^{-2} \lesssim 0.14. \quad 1.$$

If $\Omega = 1$ then the majority must be nonbaryonic.

Several suggestions have been made recently for how to avoid this constraint on Ω_b (33–35). Although clever and promising, so far none has managed to reproduce acceptable abundances for all the light nuclides.

What if the cosmological density is actually at the lower end of the observationally allowed range, $\Omega_0 \sim 0.2$? This is perhaps barely consistent

with the highest value allowed by the standard nucleosynthesis constraint, Equation 1. Such a low-density universe is potentially in conflict with the upper limits on small-angle CBR anisotropies $\delta T/T$ (25–31). This is particularly true for adiabatic scenarios, in which photon diffusion (Silk damping) destroys galaxy-scale fluctuations and galaxies must form after “pancake” collapse on larger scales. The best theory available for an entirely baryonic universe is therefore probably an isocurvature model (36).

Is it possible that the DM comprising the nonluminous halo of our galaxy and other galaxies is entirely baryonic? Perhaps, but various observational constraints (37) restrict the possible forms it may take to two: “Jupiters” (isolated planet-size gas balls too small to shine), or black hole stellar remnants of at least $10^2 M_\odot$ (since only such very massive objects would collapse to black holes with ejecting too much matter enriched in heavy elements). Although it is difficult, but perhaps not impossible (38–40), to invent schemes in which 90% of the baryonic matter in galaxies is converted to these unusual forms rather than to stars, there is still another problem. Unless this happens before the dissipative infall of the visible matter in galaxies, the solution to the angular momentum problem of spiral galaxies based on infall within dissipationless halos (10) does not work. [The nonluminous mass in the disk of our galaxy (41), if there actually is any (42), is probably ordinary matter in some form since it is most plausible that dissipative infall brought this matter to the galactic disk.] To summarize, the DM is likely to be nonbaryonic, especially if $\Omega = 1$.

1.3 *Nonbaryonic DM Candidates*

From the viewpoint of particle physics, it is quite plausible that the majority of the matter in the universe is nonbaryonic. The lightest superpartner (LSP, Section 2.1.2) and the axion (Section 3) are two particle physics DM candidates that are “well motivated,” in the sense that they are needed in particle theories that were invented to solve problems entirely unrelated to the cosmology of DM. Although these theories have been quite popular with particle theorists for several years, they remain speculative. Not only is there no direct evidence that the LSP or axion actually exists; even if one or both do exist, they might not have the right mass and interaction strength to be cosmologically dominant. Nevertheless, particle physicists were already working on these DM particle candidates for reasons of their own by the time most astronomers were convinced of the reality of DM.

Other elementary particle possibilities for the DM have also been proposed, including neutrinos both light ($m_\nu \lesssim 30$ eV; Section 4) and massive ($m_{\nu_H} \gtrsim 3$ GeV; Section 2.1.1). Some additional DM candidate particles,

called “cosmions” (Section 2.1.3), have been proposed specifically to solve the solar neutrino puzzle. Finally, there are several hypothetical particles (43)—for example, right-handed neutrinos, GUT monopoles, quark nuggets, shadow matter, preons, pyrgons, flatinos—sharing one or more of the following characteristics: they are generally regarded as even more speculative as DM candidates than the possibilities already listed; their properties are less well defined; and the prospects for their detection are bleak. We do not discuss them further here.

DM particles are generally assumed to have only weak and gravitational interactions. If they interacted strongly or electromagnetically, they would presumably have participated in the dissipative processes that led to the infall of the baryonic matter in galaxies and the formation of the galactic spheroid and disk, rather than remaining in the extended dark halo. The experimental limits (44, 45) on the terrestrial abundance of anomalous heavy isotopes are far below those expected (46) if even a tiny fraction of the DM condensed with the planets. It is natural to assume that the DM is invisible and has negligible electromagnetic interactions because it is composed of electrically neutral particles.

All DM candidate particles must have lifetimes long compared to the age of the universe, $t_0 \approx 5 \times 10^{17}$ s. This is achieved by assuming that their decay is either prevented by a conserved quantum number or suppressed by their very light mass.

A broad category of DM candidates is known as weakly interacting massive particles (WIMPs). These particles generally have masses in the range 1–100 GeV and weak [as in $SU_L(2)$] strength interactions; thus their name. Their stability is ensured by a conserved quantum number, which may be multiplicative or additive depending upon the model. We discuss the possibilities for detecting WIMPs in Section 2. Axions (Section 3) and light neutrinos (Section 4) exemplify particles stable by virtue of their small mass.

2. WEAKLY INTERACTING MASSIVE PARTICLES

2.1 *Motivation for and Properties of WIMP Candidates*

In this review we confine our discussion to three categories of WIMPs. Massive neutrinos (Section 2.1.1) are important for their historical and pedagogical significance. The best-motivated candidate from the viewpoint of particle physics is the LSP, i.e. the lightest superpartner particle (Section 2.1.2). We also discuss cosmions (2.1.3), a WIMPish solution to the solar neutrino problem.

The motivation for WIMP DM candidates arises from a combination of particle physics, astrophysics, and cosmological arguments. The main

astrophysical motivation for WIMP (or axionic) DM is the success of cold DM (8, 47–49), a theory of the origin of galaxies and large-scale structure in the universe. In all current theories of galaxy formation the structures we currently see in the universe arise from the gravitational growth of density fluctuations that are originally small in amplitude on the spatial scale of galaxies. The essential idea of cold DM is that all fluctuations larger than $\sim 10^5 M_\odot$ are preserved in the cold DM. Hot or warm DM theories have small-scale fluctuations erased by free streaming of relativistic (hot) particles (see Section 4). There are, of course, competing theories of galaxy formation where, for example, loops of “cosmic string” (50–53) act as seed masses, or gigantic explosions occur (54, 55) to initiate growth of fluctuations. In those theories DM is still needed to provide the nonluminous mass in galaxies and clusters and perhaps to make $\Omega = 1$, but it is not clear what role it plays in galaxy formation.

Within the context of cold DM, simple and plausible explanations have been given for key observational regularities of galaxies and clusters such as the variation of total mass with rotational or virial velocity, i.e. the Tully-Fisher and Faber-Jackson relations (8); for the flat rotation curves of spiral galaxies (11); for the existence and properties of Lyman α clouds (56), globular clusters (57, 58), and dwarf galaxies (59); and possibly for the origin of biasing in galaxy formation (17, 60–62). None of these issues has been seriously addressed in the hot DM picture, or in the dynamically complicated cosmic string or explosion theories. To be honest, however, we must note that cold DM may not do particular well in explaining voids in the spatial distribution of galaxies (63, 64), large-scale peculiar velocities (65–67), or spatial correlations of Abell clusters (68, 69).

A different astrophysical motivation for WIMPs is the cosmion hypothesis (70–73), in which DM particles are invoked to explain the paucity of ^8B solar neutrinos in Davis’ detector (74, 75) and the Kamiokande detector (76). WIMPs captured by the Sun become the main vehicle for energy transport in the solar core, lowering the central temperature and the production rate of ^8B neutrinos. This hypothesis requires relatively large elastic cross sections for WIMPs on ordinary matter, and negligible WIMP annihilation in the sun.

The cosmological motivation for WIMPs is that they give $\Omega_\delta \approx 1$ in a natural way.¹ The “standard” assumption is that the δ particle-antiparticle asymmetry is negligible, so that Ω_δ is determined by the annihilation cross section $\langle\sigma v\rangle_\Lambda^F$ at δ “freezeout,” the time when δ particles drop out of chemical and thermal equilibrium (77–79),

¹ We use the symbol δ (for dark) to refer to generic or particular WIMPs.

$$\langle\sigma v\rangle_A^F = (1-2) \times 10^{-26} \gamma (4\Omega_\delta h^2)^{-1} \text{cm}^3 \text{s}^{-1}. \quad 2.$$

The factor $\gamma \sim 1$ embodies cosmological uncertainties such as entropy production after freezeout, and the range 1–2 reflects uncertainties in freezeout related to details of the particular WIMP model. In Equation 2 the value of Ω does not depend explicitly on m_δ . This arises because the abundance of WIMPs after freezeout, Y_δ , is nearly proportional to $(m_\delta M_{\text{Pl}} \langle\sigma v\rangle_A^F)^{-1}$, where the Planck mass $M_{\text{Pl}} = 1.22 \times 10^{19}$ GeV. It follows that $\Omega_\delta \sim Y_\delta m_\delta$ is independent of m_δ except implicitly through $\langle\sigma v\rangle_A^F$. For most WIMPs $\langle\sigma v\rangle_A^F \sim m_\delta^2$, which results in a lower bound on m_δ so that $\Omega_\delta \lesssim 1$. It is perhaps significant that particles with m_δ of a few GeV and weak strength interactions (i.e. WIMPs) naturally give $\Omega_\delta \approx 1$. Alternatively, Ω_δ could be determined by asymmetry. A WIMP with $m_\delta = 10$ GeV and an asymmetry equal to the baryon asymmetry would also have $\Omega_\delta \approx 1$.

The logical connections between the motivations for WIMP candidates, their properties, and the schemes for detecting them are summarized in Figure 1. If Ω_δ is determined by annihilation, then knowing $\langle\sigma v\rangle_A$ allows prediction of the rate of δ annihilation in the halo of our galaxy and also of processes that can be studied at accelerators such as $e^+e^- \rightarrow \delta\delta\gamma$. Theory (crossing+ models) relates the δ annihilation cross section to the cross section σ_{el} for δ elastic scattering on ordinary matter. This in turn is important for determining both the event rates in laboratory experiments for δ detection by elastic scattering and the efficiency of δ capture by the Sun and Earth. Energetic neutrinos from the annihilation of these captured δ s could be detected in proton-decay detectors. On the other hand, if Ω_δ is determined by asymmetry there is only a lower bound on the interaction strengths such that the minority species is eliminated (80). However, the cosmion hypothesis *would* fix elastic scattering cross sections and imply direct detection rates.

2.1.1 MASSIVE NEUTRINOS The first sort of DM particle candidate to be investigated was a massive neutrino (77–79). As a WIMP with simple, well-defined characteristics, it serves a useful role in making calculations explicit that would otherwise remain vague in their model dependency. However, it is not well motivated from the point of view of particle physics. A several-GeV neutrino would require a very large mass splitting from the three known neutrinos, and in order to be stable on cosmological time scales it must be orthogonal to the e , μ , and τ neutrinos to better than one part in 10^9 .

Two varieties of massive neutrinos are possible, Dirac (ν_D) and Majorana (ν_M). Dirac neutrinos have four spin states. It is usually assumed that there are no right-handed currents, so ν_D interacts with the V-A neutral

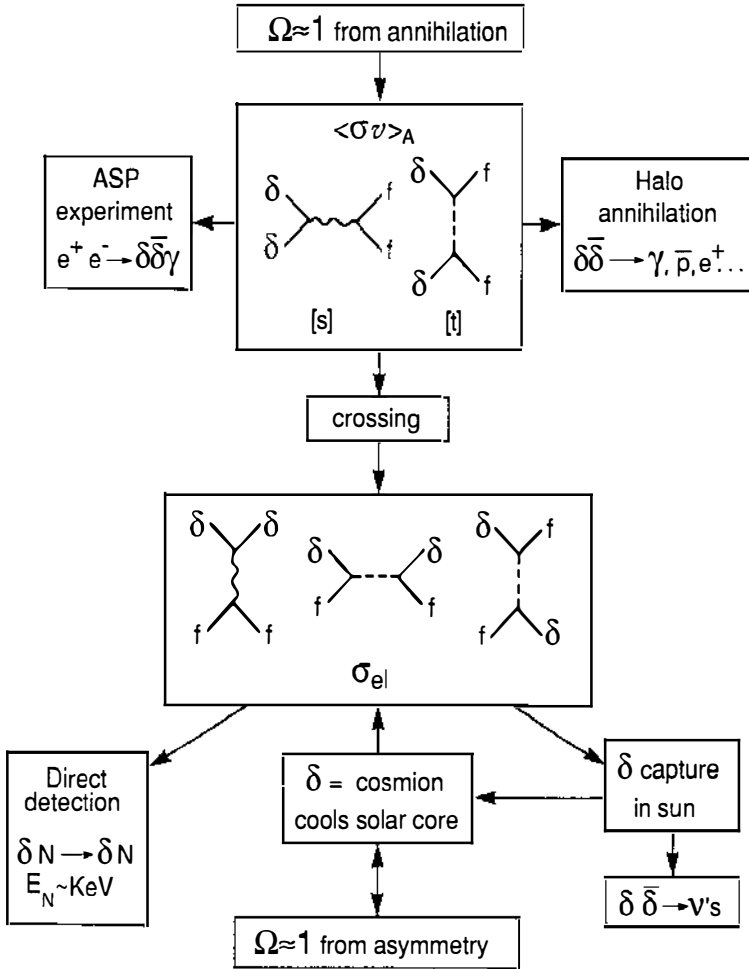


Figure 1 WIMP DM logic (see text for discussion).

currents appropriate to uncharged particles. Dirac neutrinos carry an additive lepton number and may therefore possess a cosmological asymmetry. Majorana neutrinos have only two spin states. They are their own antiparticles in the sense that nonrelativistic ν_M may annihilate with each other. Such WIMPs could only be stable as a result of a multiplicative quantum number. Since the two chirality states carry opposite vector charges, nonrelativistic Majorana particles interact predominantly through axial currents and couple to the spin of nuclei (81). To achieve $\Omega_\delta \lesssim 1$ requires $m_\nu \gtrsim 4$ (7) GeV for ν_D (ν_M) (77, 80, 82).

2.1.2 LIGHTEST SUPERPARTNER The lightest superpartner (LSP) is a DM WIMP that arises naturally in most supersymmetry theories (83–88).

Supersymmetry (89) is attractive to particle theorists for at least two reasons, aesthetics and the possibility that it can resolve the hierarchy problem (90). Moreover, supersymmetry may be a necessary feature of any quantum theory of gravity. It is based on the idea that there should be a fundamental symmetry in nature between fermions and bosons. In supersymmetry, there is one superpartner particle state for every ordinary particle state, with the following terminology. If the ordinary particle is a boson, for example, the photon (γ) or Higgs boson (h), its fermionic superpartner has the same name with *-ino* added (and a tilde over its symbol): photino ($\tilde{\gamma}$), higgsino (\tilde{h}). If the ordinary particle is a fermion, for example, an electron neutrino (ν_e), its superpartner's name has a prefix *s-*: electron sneutrino ($\tilde{\nu}_e$).

Most supersymmetry theories contain a reflection symmetry known as *R*-parity (91, 92), $R = (-1)^{3(B-L)}(-1)^{2S}$, where *B* and *L* are baryon and lepton numbers, respectively, and *S* is spin. *R*-parity is therefore an exact symmetry in any theory in which (*B* - *L*) is conserved, for example. Effects that could break *R*-parity are severely constrained by experiment (93-95) or cosmological arguments (96). Under *R*-parity, all ordinary particle fields are unchanged and all superpartner fields change sign. Conservation of *R*-parity therefore implies that an initial state containing a superpartner particle can only evolve into a final state with an odd number of such particles. Hence the LSP is stable. Because of the limits on anomalous heavy isotopes (44, 45), in any acceptable theory the LSP must be an electrically neutral color singlet. This limits the LSP to being either a mixture of neutral Majorana fermions $\tilde{\gamma}$, \tilde{h} , and \tilde{Z} ; or a $\tilde{\nu}$; or possibly a gravitino $\tilde{g}_{3/2}$ (83, 84, 97). The $\tilde{g}_{3/2}$ is not the LSP in currently favored supersymmetric phenomenology, and because of its small cross sections it would be difficult to detect, so we do not discuss it further here.

The mass of the LSP remains an open question, although if supersymmetry is invoked to solve the hierarchy problem one expects superpartner masses to be associated with the weak scale. Since the LSP is the lightest of these new particles, it is not unreasonable to postulate masses in the range of a few GeV to tens of GeV. Experimental limits are rather indirect. If produced in accelerator experiments, charged or colored superpartners could be readily detected, and so lower limits on their masses can be obtained (98). However, although neutral LSPs may be produced, they will not be directly detectable. Their production must be inferred from missing-energy experiments, such as "monojets" at $p\bar{p}$ colliders (98a) or anomalous single-photon (ASP) events at an e^+e^- machine (99). A combination of experimental data from the ASP experiment and the requirement that the universe not be overclosed suggests that a pure photino must have mass $m_{\tilde{\gamma}} \gtrsim 2$ GeV (86). However, in general the LSP

may be a linear combination of $\tilde{\gamma}$, \tilde{h} , and \tilde{Z} , and we know of no general limits on its mass. It is even possible that a light ($m_\delta < 100$ eV) LSP closes the universe (100, 101), although such models may run afoul of constraints derived from consideration of the neutrino signal from supernova SN87a (102).

The other possibility for the LSP is a sneutrino. The $\tilde{\nu}$ annihilation rate is usually semiweak rather than weak because it is mediated by the \tilde{Z} , a fermion, with amplitude proportional to $m_{\tilde{Z}}^{-1}$ rather than $m_{\tilde{Z}}^{-2}$. In this case $\langle \sigma v \rangle_A$ is independent of m_δ and there is no lower limit on the $\tilde{\nu}$ mass from the cosmological density (87, 88). In fact, to achieve $\Omega_\delta = 1$ requires some suppression of \tilde{Z} exchange, which in turn suggests a light higgsino. In that case, if sneutrinos are to constitute the DM and still be the LSP, then $m_\delta \lesssim 4$ GeV (87, 88). It is also possible to suppress \tilde{Z} exchange by making all the neutralinos very heavy (103). In this case, $\Omega_\delta = 1$ implies $m_{\tilde{\nu}} \approx 7$ GeV.

2.1.3 COSMIONS The cosmion (solar WIMP) solution (70–73) to the solar neutrino problem is quite remarkable and also fairly predictive of WIMP properties. The cosmion solution requires a population of WIMPs in the Sun's core to act as an efficient transporter of heat, isothermize the core, and thereby reduce the emission rate of ^8B neutrinos. In order to maximize the heat transport, the cosmion should interact with the solar material about 20 times per orbit around the core (73a). This suggests a critical value for the elastic cross section per baryon of solar matter, $\sigma_{\text{crit}} \approx (1-10) \times 10^{-36}$ cm². With this cross section the cosmion solution requires an abundance of 10^{-11} cosmions per baryon of solar material (a smaller or larger cross section would require a higher abundance of cosmions). It is a remarkable coincidence that if the DM is made of WIMPs, the ratio of the number of WIMPs that have struck the Sun in its lifetime, $\sim 10^{46}$, to the number of baryons in the Sun, 10^{57} , is also about 10^{-11} . Thus, if their elastic cross section is $\sigma_{\text{el}} \gtrsim \sigma_{\text{crit}}$, then nearly all the WIMPs that struck the Sun were accreted, and the concentration required to isothermize the solar core and hence solve the solar ν puzzle is achieved. In order for the cosmion solution to work, the cosmion mass must be in the range $4 \lesssim m_\delta \lesssim 10$ GeV. If $m_\delta \lesssim 4$ GeV, competition between capture and evaporation (80, 104) will determine an equilibrium abundance of cosmions too low to solve the solar ν problem, although for $\sigma > \sigma_{\text{crit}}$ evaporation from the core may be suppressed. If $m_\delta \gtrsim 10$ GeV, they will orbit too close to the center of the Sun for them to affect enough of the solar core to solve the solar ν puzzle (105).

None of the LSP candidates works as a cosmion, since the elastic scattering cross sections σ_{el} are too small (106). An additional problem is

that their annihilation rate increases with their concentration in the solar core, and this prevents the buildup of a sufficient concentration for isothermalization (106). Nevertheless, it is possible to construct cosmion candidates that simultaneously provide the DM and solve the solar ν problem (107–109). Perhaps it is best to regard these models primarily as existence proofs that a cosmion is not inconsistent with any known particle physics and cosmology. In any event, since the cosmion has relatively strong couplings to matter, the next generation of laboratory WIMP searches will either find cosmions or rule them out (see Section 2.3.3).

2.2 Interaction Rates of WIMPs with Ordinary Matter

In order to evaluate the proposed WIMP detection techniques, one must know the relevant cross sections. To determine the interaction rates one also must know the phase-space density of the WIMPs. For the indirect schemes that depend upon detection of WIMP annihilation products, one must know the yield of the product per annihilation event. Since much of this material is common to all of the proposed experiments, we describe the more general features here, and leave till later those details specific to a given experiment.

2.2.1 CROSS SECTIONS We discuss general considerations that determine the cross sections, but leave many details to the references. In this spirit, Table 2 contains general information for the WIMP candidates discussed in Section 2.1, including reference to more detailed work on particular WIMPs. Columns 1 and 2 identify the WIMP and its status as a Majorana fermion. Columns 3 and 4 identify the possible intermediate particles for s- and t-channel annihilation. Elastic scattering processes are related to annihilation by “crossing,” as illustrated in Figure 1. Columns 5 and 6 are relevant for annihilation rates in the universe today. Columns 7 and 8 contain information on elastic WIMP nucleus cross sections, and the last column contains references to relevant papers.

If there is no cosmic asymmetry, then the annihilation cross section at freezeout, $\langle\sigma v\rangle_{\text{A}}^{\text{F}}$, is determined by Equation 2. More generally, it is useful to approximate the annihilation cross sections by the form (86) $\langle\sigma v\rangle_{\text{A}} = a + b\langle v^2\rangle$, where the angle brackets denote phase-space averaging and v is the relative velocity between the two WIMPS. During freezeout $\langle v^2\rangle = 6T/m_{\delta} \sim 1/4$, whereas for annihilation in either the galactic halo or the Sun $\langle v^2\rangle \sim 10^{-6}$. If m_1 is the mass of the intermediate particle, and g_{δ} (g_f) is a typical coupling for the intermediate particle to the WIMP (annihilation product f) then dimensional analysis would suggest $a \sim b \sim g_{\delta}^2 g_f^2 m_{\delta}^2 / m_1^4$. For Majorana fermions this analysis breaks down (85); the s-wave piece is suppressed for annihilation into light particles

with mass m_τ , i.e. $a \sim (m_\tau/m_\delta)^2 b$. If the WIMP mass is close to some threshold then the annihilation cross section today, $\langle\sigma v\rangle_A^0$, may be similar to that at freezeout, $\langle\sigma v\rangle_A^F$, but if m_δ is more than a factor of two away from all thresholds, then $\langle\sigma v\rangle_A^F$ is determined by the b coefficient while $\langle\sigma v\rangle_A^0$ will be determined by the a coefficient. Thus, for Majorana WIMP masses in the range 3–5 GeV and greater than 10 GeV, annihilation in the galactic halo is suppressed. For non-Majorana fermions we expect $a \sim b$ and so $\langle\sigma v\rangle_A^0 \sim \langle\sigma v\rangle_A^F$.

On the other hand, if the abundance today is determined by an initial asymmetry, then only a lower bound may be placed on the cross sections from requiring that annihilation be efficient enough to eliminate the minority species. We note that Majorana fermions cannot support a particle-antiparticle asymmetry, while most cosmion candidates require one in order to achieve sufficiently high elastic cross sections within the solar interior and still be abundant today (see, however, 107). There exists the possibility of a $\tilde{\nu}$ asymmetry; however, it seems unlikely that it would play an important cosmological role.²

For low-energy elastic cross sections, dimensional analysis plus kinematics give

$$\sigma_{\delta N} \sim g_\delta^2 g_N^2 \frac{m_\delta^2 m_N^2}{(m_\delta + m_N)^2} \frac{1}{m_1^4}, \tag{3}$$

where m_N is the mass of the nucleus (81). The coupling to the nucleus, g_N , depends strongly on whether the WIMP is a Majorana fermion. Because of the small velocities and momentum transfers, the nucleus acts coherently as a scatterer. Thus, for a particle with vector couplings, the “charge” of the nucleus is the sum of the charges of the constituents. Unless there is a remarkable cancellation, $\sigma_{\delta N}$ grows as the square of the atomic weight in addition to the kinematic factors.

Majorana fermions, on the other hand, have primarily axial vector couplings, so at low momentum they couple to nuclei through a spin-spin interaction (81). In most nuclei, most of the nucleons have their spins sum pairwise to zero and therefore the “charge” of the nucleus does not increase with the size of the nucleus. The spin content of nuclei depends upon the nuclear wave functions, and also upon the spin wave functions of the quarks inside the individual nucleons (81). The first problem has been

²The $\tilde{\nu}$ asymmetry is $\Delta y_{\tilde{\nu}} \sim 10^2 \Delta y_L y_{\tilde{\nu}}$ where Δy_L is the lepton asymmetry and $y_{\tilde{\nu}} = n_{\tilde{\nu}}/s$ is the sneutrino number density divided by the entropy density when $\tilde{\nu}\tilde{\nu}$ annihilation freezes out (80). If Δy_L is of the same order as the baryon asymmetry, then $\langle\sigma v\rangle_{\tilde{\nu}\tilde{\nu}}$ must be $\lesssim 10^{-7} \langle\sigma v\rangle_{\tilde{\nu}\tilde{\nu}}$ in order for $\Delta y_{\tilde{\nu}}$ to be significant. Even if $\Delta y_L \sim 1$, $\langle\sigma v\rangle_{\tilde{\nu}\tilde{\nu}} \lesssim 10^{-6} \langle\sigma v\rangle_{\tilde{\nu}\tilde{\nu}}$ to suppress a solar $\tilde{\nu}\tilde{\nu}$ annihilation signal, although observable halo annihilation signals would be suppressed for any $\langle\sigma v\rangle_{\tilde{\nu}\tilde{\nu}}$ if $\Delta y_{\tilde{\nu}}$ is significant.

¹ Setting $\Omega_\delta h^2 = \frac{1}{4}$ and using EMC data ($g_{Ap} = 1.48$).

Assuming no asymmetry.

$$N = \left(\frac{m_\delta m_N}{m_N + m_\delta} \right)^2.$$

$$Z_N = N_N - (1 - 4 \sin^2 \Theta_w) Z_N, \sin^2 \Theta_w = .226 \pm .004$$

$N_N = \#$ of neutrons in N , $Z_N =$ charge of N .

$$= 2\lambda_N \sum_q T_q^3 \Delta q, \text{ where } \lambda_N = \left[\frac{J(J+1) + S(S+1) - L(L+1)}{\sqrt{3}J(J+1)} \right]$$

for single particle shell model and $J =$ nuclear spin, $S = \frac{1}{2}$, $L = J \pm \frac{1}{2}$, \sum_q is sum over quark flavors, T_q^3 is isospin of quark,

and Δq is the spin of the nucleon carried by quark flavor q . For the naive quark model $\Delta u = 0.97$, $\Delta d = -0.28$, $\Delta s = 0$, $g_{Ap} = 1.25$. Using the EMC results $\Delta u = 0.74 \pm 0.08$, $\Delta d = 0.51 \pm 0.08$, $\Delta s = -0.23 \pm .08$; $g_{Ap} = 1.48$, $g_{An} = 1.02$.

$$m_\delta = 4 \text{ GeV.}$$

^g $S_f \sim B_f \left(\frac{m_f}{m_\delta} \right)^2$ where B_f is the branching ratio at freezeout for annihilation into the heaviest fermion such that $m_f < m_\delta$.

^h $m_\delta = 7 \text{ GeV.}$

ⁱ $\lambda_N, \Delta q$ as in e ; Q_q is charge of quark q , $e^2 = 4\pi\alpha$. This form assumes left and right squark masses are equal.

^j $m_\delta = 10 \text{ GeV}$, $m_q = 84 \text{ GeV.}$

^k $\tan(\beta) = v_1/v_2$, the ratio of two higgs vevs. This form neglects Yukawa couplings to the quarks.

^l $m_\delta = 10 \text{ GeV}$, $\cos^2(2\beta) = \frac{1}{2}$.

^m Generic "LSP" is a linear combination of all neutral spin $\frac{1}{2}$ particles: $\tilde{\gamma}, \tilde{z}, \tilde{h}_1, \tilde{h}_2$.

ⁿ $\tilde{W}, \tilde{\ell}$ exchange are less important.

^p $m_\nu = 4 \text{ GeV}$. Note that capture in the sun will be dominated by ${}^4\text{He}$, where $g_\nu \approx 1.8$.

treated in a simple single-particle shell model (81, 110, 111), but this technique is inadequate for many nuclei. The second problem has been treated (103, 111, 112) using experimental data from neutron and hyperon decays and either theoretical input based upon the “naive quark model” or data from the European Muon Collaboration (EMC) experiment, where polarized muons were scattered from a polarized target (113). Unfortunately, the different approaches give different results. Using the naive quark model an accidental cancellation occurs that suppresses the coupling of photinos to neutrons by two orders of magnitude. Given these uncertainties, it would be wise to design direct detection experiments so that a variety of materials may be used as the target.

Griest (114) has recently found that there can be a scalar part to the elastic cross section for Majorana fermions on nuclei, if the LSP is not a pure $\tilde{\gamma}$, \tilde{h} , or \tilde{Z} . This means that spinless nuclei may become viable targets.

Exceptions to the above comments are sneutrinos ($\tilde{\nu}$) (87, 88) and most of the cosmion candidates (107–109). As mentioned in Section 2.1.2, $\tilde{\nu}$ annihilation is usually dominated by \tilde{Z} exchange to two neutrinos, in which case $\langle\sigma v\rangle_A \sim g_s^2 g_f^2 m_1^{-2}$. For the cosmions some “exotic” physics is required to get σ_{el} significantly larger than “weak”; for example, in the magnino model (108), the intermediate particle is a photon, there is no suppression by m_1 , and cross sections are determined by the magnetic moment of the magnino.

We emphasize that, although much progress has been made, there is considerable uncertainty in the cross sections. For Majorana WIMPs, determining the spin content of nuclei can lead to uncertainties in σ_{el} that can be as big as an order of magnitude. For annihilation, a number of approximations have been made that make the calculations easier to perform and utilize. The situation is especially bad for the LSP candidates, where model dependence introduces substantial uncertainties into all cross sections (86, 111, 114).

In order to give a widely applicable discussion of possible experiments, we find it convenient to define fiducial cross sections: $\langle\sigma v\rangle_{A26} \equiv \langle\sigma v\rangle_A/10^{-26} \text{ cm}^3 \text{ s}^{-1}$ for annihilation, and $\sigma_{\delta N38} \equiv \sigma_{\delta N}/10^{-38} \text{ cm}^2$ for elastic scattering from a nucleus N.

2.2.2 PHASE-SPACE DENSITIES The phase-space density of WIMPs in the Galaxy is a crucial input to event rate calculations. The dynamical considerations that lead us to postulate DM also suggest that the DM distribution may resemble

$$\rho = \rho_0 \frac{a^2}{a^2 + r^2}, \quad \frac{dn}{dv} = A \frac{n_0 v^2}{\sigma_H^3} \exp\left(-\frac{v^2}{\sigma_H^2}\right), \quad v < v_e, \quad 4.$$

where ρ_0 , a are the halo core density and radius, σ_H is the halo velocity dispersion, v_e is the position-dependent escape velocity from the Galaxy, and $A = 4/\sqrt{\pi}$ for $v_e \gg \sigma_H$. Using a distance from the Sun to the center of the Galaxy $r_\odot = 8.5$ kpc (115) and a circular velocity at large radii $v_\infty = 213$ km s⁻¹ (116a,b), we follow Flores (117) and deduce nominal values

$$\rho_0 = 1.0 \text{ GeV cm}^{-3}, \quad a = 5.6 \text{ kpc}. \quad 5.$$

We appeal to (116a) to set $v_e = 640$ km s⁻¹ and find $\sigma_H = 213$ km s⁻¹.

For many experiments we need only the local DM density, ρ_\odot . The values in Equation 5 lead us to the fiducial $\rho_{.3} \equiv \rho_\odot/0.3$ GeV cm⁻³.

The rms halo velocity for this halo model, $\langle v^2 \rangle^{1/2} = 261$ km s⁻¹, is not always a useful fiducial. For example, for direct detection we are interested in $\langle v \rangle$, while for capture in the Sun $\langle v^{-1} \rangle$ is needed. These average values must be calculated in the proper reference frame, including effects due to the Sun's motion through the halo (119), the Earth's motion around the Sun (110, 120, 120a), and the gravitational potentials of the Sun and Earth (120, 120b); see Section 2.3.2.2. For convenience, in the equations below we scale the relevant velocity averages to 300 km s⁻¹ but give the more exact values where known.

The isothermal sphere halo model discussed above is at best a rough approximation. The true form of the halo may depend upon the details of its formation in a fairly complex way. It is likely that the velocity distribution at the Sun's position in the Galaxy will be considerably flatter (123) than the Boltzmann distribution in Equation 4. Further, although at large radii the $1/r^2$ density profile is determined by rotation curves, in the inner regions of galaxies baryonic matter dominates the dynamics and the form in Equation 4 is strictly a matter of convenience.

2.2.3 YIELDS For the indirect signals resulting from WIMP annihilation one must know the yield $\langle N_i \rangle$ of detected annihilation product "i" per event. A reasonably good way to obtain this value is to use data from high-energy e^+e^- scattering experiments (124–126). The rationale is that the hadronization of a quark-antiquark pair should not depend on how that pair was formed. The problem is that DM annihilation will presumably have branching ratios to produce $b\bar{b}$, $c\bar{c}$, etc that are different from those in e^+e^- events. If the yields depend sensitively on the quark flavor, substantial errors may ensue. One remedy is to use an event generator, such as the LUND program (127), and Monte Carlo yields for different flavor fermions. In doing this, one must take care that the event generator has been "tested" for the signal in question. For example, using

a program to predict the results of annihilation into top quarks involves an extrapolation of our knowledge.

2.3 Direct Detection by Nuclear Recoil

The exciting possibility exists of detecting WIMPs in the laboratory (81, 128). The idea is that in an elastic collision with a nucleus the WIMP may impart a few keV of energy to the nucleus. That energy might be detected via a small current arising from ionization, as a small increase in temperature, or perhaps as a shower of phonons, all from the recoil nucleus. In the rest of this section we discuss the rates such an experiment might achieve, the chief sources of background, and the current status and prospects for the various detector technologies.

2.3.1 EVENT RATES The rate for elastic scattering in a laboratory detector is

$$R = 4.3 \frac{X_N}{m_N m_\delta} \sigma_{\delta N 38} \rho_\odot \langle v_{300} \rangle \text{ kg}^{-1} \text{ day}^{-1}, \quad 6.$$

where $\sigma_{\delta N 38}$ is the elastic WIMP-nucleus cross section in units of 10^{-38} cm^2 and ρ_\odot is the halo density scaled to our fiducial value (Section 2.2.2). For our fiducial halo, taking into account the Sun's gravitational potential and motion (120, 120a), the mean speed at a detector on Earth is $\langle v_{300} \rangle = 1.04$. The rate is given per unit detector mass, and so it is inversely proportional to the mass of the target nucleus m_N (in GeV), and proportional to the fraction of the detector mass in the target species, X_N . The recoil energy of the struck nucleus is

$$\Delta E = \frac{m_N m_\delta}{(m_N + m_\delta)^2} m_\delta v^2 (1 - \cos \theta), \quad 7.$$

where v is the velocity of the incoming WIMP and θ is the center-of-mass scattering angle. All of the WIMPs in Table 2 (except the magnino) have isotropic differential elastic cross sections, and so for a given WIMP velocity the differential event rate is flat from $E = 0$ to $E_{\max} = \Delta E(\theta = \pi)$. The total differential rate is given by integrating over the phase-space distribution of the WIMPs.

As discussed in Section 2.2, the value of $\sigma_{\delta N}$ varies greatly depending upon the WIMP and the target nucleus due to the kinematic factor $[m_\delta m_N / (m_\delta + m_N)]^2$ as well as the details of the matrix element. In Figure 2 we show plausible event rates for two candidate WIMPs as a function of m_δ , for a variety of target nuclei (121). The photino detection rates in Figure 2 (*top*) assumes equal squark and slepton masses adjusted so that $\Omega_\delta h^2 = 0.25$, and use the nuclear matrix elements of Ellis & Flores (111)

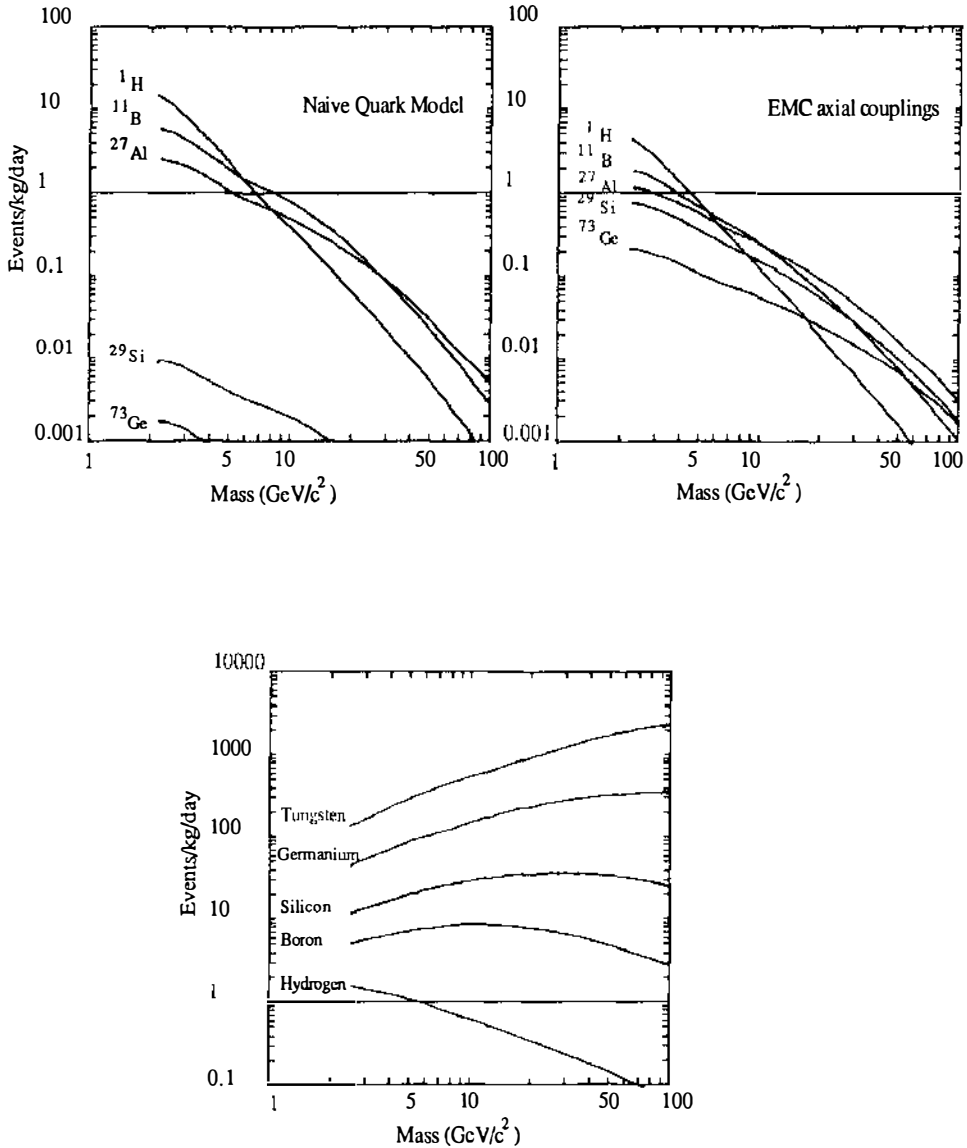


Figure 2 Interaction rates of WIMPs (assumed to form the DM halo of our Galaxy) vs mass for various target materials, (top panels) for $\Omega_{\text{DM},0} \approx 1$ from annihilation survival, and (bottom panel) for $\Omega_{\text{DM},0} \approx 1$ from asymmetry. In the top panels, the assumed WIMP is a pure photino, the sfermions are assumed to be degenerate with their mass determined so that $\Omega_{\tilde{\gamma}} h^2 = 0.25$, $\rho_0 = 0.3 \text{ GeV cm}^{-3}$, $v_0 = 230 \text{ km s}^{-1}$, and $\langle v_{\text{halo}}^2 \rangle^{1/2} = 270 \text{ km s}^{-1}$. In the top left and right parts of Figure 2, the axial couplings are determined from the naive quark model (left) and the recent European Muon Collaboration measurements (right), as discussed in (111). In the bottom panel, the WIMP is a heavy Dirac neutrino ν with hypercharge $\frac{1}{2}$ interacting via Z^0 exchange. (This model requires a $\nu - \bar{\nu}$ asymmetry for m , above a few GeV.) The halo parameters are the same as in the top panels.

assuming their NQM or EMC-derived axial charges. Figure 2 (*bottom*) shows event rates for a massive Dirac neutrino assuming $\Omega_\delta = 1$ from cosmic asymmetry. The event rates are much larger because of the vector coupling to the nucleus. Cosmions have even larger rates. It should be clear that detecting $\tilde{\gamma}$ or \tilde{h} DM will be the more formidable problem.

2.3.2 BACKGROUNDS AND SIGNATURES The basic experimental problem is to extract from the background the rather small signals predicted in Equation 6.

2.3.2.1 Backgrounds We have to distinguish among three background sources:

1. Cosmic rays can be vetoed, and they deposit so much energy that they can easily be rejected. However, even though their rate at sea level is not high, event overlap problems may arise for very slow detectors, such as thermal detectors with very long time constants. Moreover, the indirect effects—spallation products and neutron production by muon capture—can generate relatively large radioactive backgrounds in the detector. These two reasons will probably force DM search experiments to be located deep underground.

2. The main background will come presumably from the residual radioactivity in the detector elements and in their surroundings. Internal radioactivity of the detectors is expected to be negligible if crystals such as Ge, Si, and maybe B are used. Some doubts have been expressed about silicon (129), which could be contaminated by ^{32}Si . This seems unlikely for silicon originating in deep mines (130). On the other hand, spallation products such as ^{68}Ge (131) or tritium (132), produced during the time the detector elements are exposed to the cosmic radiation at the surface of the Earth, may be quite disturbing because the decay energy is in the range of interest. Tritium is particularly annoying because of its low β energy and long lifetime, and it may have to be displaced with ordinary hydrogen (132). The main source of background will presumably be the surroundings (refrigerator, dewar, shield). The α and β particles can be eliminated by imposing a fiducial region. Fast neutrons from U and Th decays or μ captures are potentially dangerous but can be thermalized easily with 40 cm of water. Slow neutrons, which may create γ rays, can be absorbed by a borated shield. By far the most difficult background to deal with is the γ rays from lines, n- γ reactions, and β bremsstrahlung. They produce a flat Compton background that may be quite difficult to decrease appreciably even with an active veto. For instance a 20-cm NaI veto has an efficiency of only 92% at a parent γ energy of 3 MeV. Another potentially dangerous mechanism is feed-down from high energy to low energies because of defects of the detector: bad collection efficiency, dead regions, edge effects,

etc. This could produce in some instances an energy spectrum peaked at low energy, like the expected signal. Localization of the interaction is essential to set up fiducial regions in the detector and reject events in regions of doubtful sensitivity. In principle this feed-down can be checked by artificially increasing the radioactive background.

3. Close to the threshold, the upper end of the electronics noise may also simulate a DM signal. Care should be taken to prevent any non-Gaussian tail in the response of the detector to a delta function, e.g. spurious signals generated by vibrations (“microphonics”), baseline variation. This response function can in principle be measured with artificial electronic pulses.

These three types of effects are seen in the double β -decay experiments of LBL/UCSB (131) and PNL/USC (133). The two groups have published background rates of the order of 0.5 to 1 event/kg/keV/day at 20 keV. This level of radioactivity is quite compatible with the expected Compton background, but may also be partially due to dead regions in the detectors. The peaks and rise observed below 20 keV are related to specific instrumental problems (radiogenic components in the detector, microphonics), which both groups think can be resolved. The two collaborations are currently attempting to decrease their thresholds. This state of the art is quite encouraging since the experiments were not designed for these low energies. The background performances of the detectors are still improving rapidly, which shows that the limit of technology is not yet reached. However, cryogenic detectors running in the less controlled environment of a refrigerator and reaching lower thresholds may encounter difficult new problems.

2.3.2.2 Signatures If a low-energy signal is observed, how can one be sure that it is from DM interactions and not from a misunderstood behavior of the detector?

1. The most unambiguous evidence would be changes in the event rate and the spectrum of energy deposition with the time of the year (120, 120a, 129). The DM halo has not collapsed significantly and is predicted to have a very small overall angular velocity. Figure 3a shows how the 30 km s^{-1} orbital velocity of the Earth around the Sun is oriented with respect to the 220 km s^{-1} orbital velocity of the Sun around the center of the Galaxy, a combination causing net velocity of the Earth through the halo to vary during the year. Because of the 60.2° tilt of the Earth’s orbit (ecliptic) with respect to the galactic plane, half the Earth’s velocity is added to (subtracted from) the Sun’s velocity in the summer (winter). The corresponding annual modulation is demonstrated in Figure 3b (from 121). The mean energy deposition varies by about $\pm 4.5\%$ and the rate varies by about

$\pm 2.5\%$. In order to observe such an effect at 3σ , about 4000 events are needed. Therefore very massive detectors (of the order of 10 kg) will be required for the unambiguous detection of LSPs in a reasonable amount of time (2 years).

There has been some confusion in the literature stemming from the fact that the modulation in the rate is higher at high energy deposition. The argument was then that relatively high threshold detectors without any energy resolution capability were sufficient. However, as the deposited energy increases, the event rate goes down rapidly, and with it the statistical sensitivity. Therefore, it is advantageous to have reasonably low thresholds to detect this effect (120a, 121). Monitoring the parameters that may fake a low-energy peak, and showing that they do not have the same periodic behavior, would provide a powerful argument for an astronomical origin.

2. The measurement of the direction of the scattered nucleus would be another powerful discrimination tool (134). This is extremely difficult. It

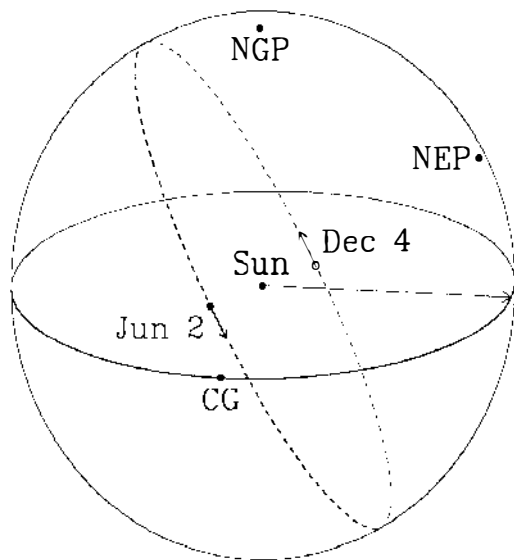


Figure 3a Annual effect in WIMP detection by elastic scattering. Why is it expected: The solid line (darker in the front) shows the plane of the galactic disk and the Sun's orbit; the dashed circle is the orbit of the Earth (ecliptic plane). NGP and NEP are the north galactic and ecliptic poles. CG shows the direction toward the galactic center, and the long and short arrows show the Sun's and the Earth's velocities. The sum of the Sun's and Earth's velocities reaches its maximum on June 2 (248 km s^{-1}) and its minimum on December 4 (219 km s^{-1}). (These velocities with respect to the galactic center are obtained neglecting the small eccentricity of the Earth's orbit, and assuming that the Sun's peculiar velocity is 16.5 km s^{-1} in the galactic direction $l = 53^\circ$, $b = 25^\circ$ with respect to the local standard of rest (cf 116). Event rates in WIMP detectors actually depend on the Earth's velocity with respect to the DM halo, whose rotational velocity is uncertain.)

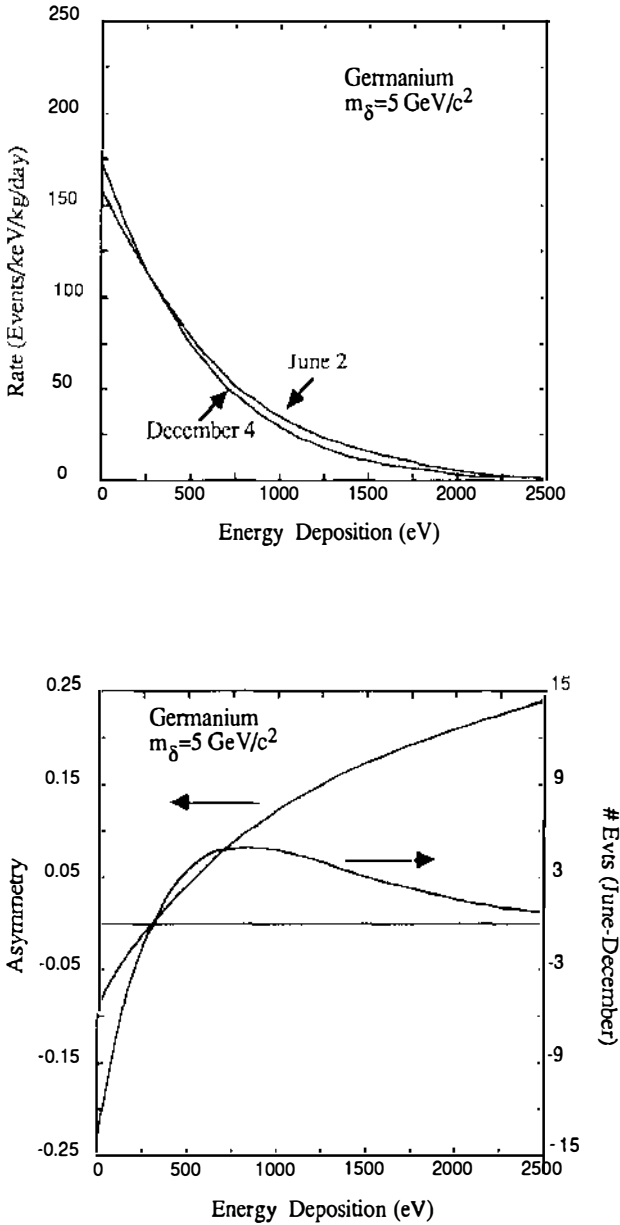


Figure 3b Annual effect in WIMP detection by elastic scattering. Rate for June 2 and December 4 vs deposited energy is shown in the top panel. The June-December difference (right axis) and asymmetry (left axis) vs deposited energy are shown in the bottom panel. Note that although the asymmetry increases with the energy deposition, the rate and therefore also the June-December rate difference both decrease at high energy deposition.

seems excluded in a solid where the range of the recoiling nuclei may not be larger than a few tens of angstroms. A remote possibility is that the ballistic phonons produced keep a memory of the initial direction of the momentum (in spite of umklapp processes!). Rich & Spiro (135) have suggested that the use of a gas at low enough pressure may indeed provide a rough directionality (see Section 2.3.3.2). It would be desirable to be able to distinguish the beginning from the end of the "track" left by the scattered nucleus, although even knowing the axis but not the direction may be useful.

3. The shape of the spectrum is an important datum. To take a simple example, spectra in germanium contaminated by ^{68}Ge show gallium, zinc, and copper x-ray lines between 8.9 and 10.6 keV that cannot be confused with a potential signal for a detector with appropriate energy resolution (131). Such a line would be fatal, however, for a "threshold" detector such as superconducting granules run in a mode providing only a yes-no answer. For such detectors, the threshold will have to be varied in order effectively to measure the spectrum. This may be too time consuming for such experiments, which are essentially rate limited. The experience of double β experiments (137) has also shown that the radioactive background of two similar detectors is usually not the same. It is therefore important to have several detectors and show that they give the same spectrum.

4. Another important indicator is the behavior as a function of the material. The energy deposition is given by Equation 7. Measuring the energy deposition in targets made of different materials will effectively allow the measurement of m_β . A neutron-induced signal can readily be identified through this mass measurement, and Compton energy deposition is independent of m_N . However, the cross section and the impurity level will vary with the element, and the rate may be too small for some of them; this obviously complicates the interpretation.

5. As emphasized above, an important discriminant against background is the spatial distribution of the energy in the detectors.

6. Another important signature would be to know that the interaction has occurred on a nucleus and not on an electron, as would be the case for β or γ interactions. This in principle can be deduced from a simultaneous measurement of ionization and heat (see Section 2.3.4.3 below).

7. In addition to elastic scattering, it has been proposed (81) that inelastic processes $\delta N \rightarrow \delta N^*$ followed by the deexcitation of the nucleus N^* would provide two coincident signals, which would be a powerful discriminant against background. Unfortunately, this rate is unlikely to exceed 10^{-4} events $\text{kg}^{-1} \text{day}^{-1}$ (138).

In conclusion, although we cannot turn off the source nor locate its direction, a fair number of tests could be used to validate a signal! As is

usual for difficult experiments, a maximum amount of redundancy has to be included in the design.

2.3.2.3 *Scaling laws* If the observed background is flat in energy, experiments searching for DM particles may run into signal-to-noise problems if the interesting range from m_δ is pushed up. If the annihilation rate at freezeout determines the present abundance of DM (i.e. there is no initial asymmetry), the integrated elastic rate is

$$S \propto \frac{m_N}{m_\delta(m_\delta + m_N)^2}, \tag{8}$$

while, if the background is flat, the noise B will be proportional to the energy range over which to integrate, that is

$$B \propto \frac{m_\delta^2 m_N}{(m_\delta + m_N)^2}. \tag{9}$$

Thus, the signal-to-noise ratio S/B goes down as m_δ^{-3} and the statistical accuracy S/\sqrt{B} goes roughly as m_δ^{-2} at large masses!

2.3.3. DETECTION METHODS I: IONIZATION DETECTORS In this section on “conventional” ionization detectors and the following section on cryogenic detectors, we review the DM detection methods that have been proposed. Table 3 summarizes this discussion.

2.3.3.1 *Energy deposition mechanism* Let us consider a detector made of gas (e.g. a proportional chamber) or of a solid crystal (e.g. a germanium detector). A DM particle is expected to interact elastically with a nucleus in the target, and the energy is deposited in the gas or the crystal by the recoiling nucleus. However, the struck atom is usually not ionized after the primary collision and only transfers part of its energy to ionization in subsequent collisions with other atoms in the medium. This process is not very efficient because of the mass mismatch between the nucleus projectile and the electron target. The resulting pulse height in an ionization detector of a slow nucleus is much smaller than that of an electron of the same kinetic energy. Sadoulet et al (130) have reviewed the experimental situation for germanium and silicon. Although there is a clear need for measuring the ionization yield at low recoil energy (this measurement is planned by two experimental groups in the coming year), data are consistent with Lindhard’s theory (139): for instance, in germanium a Ge nucleus of 12 keV has the same ionization yield as an electron of 4 keV. Calculations for gas using the measured atom-atom elastic scattering and ionization cross section (T. Shutt and B. Sadoulet, work in progress) show similar effects, with a dramatic drop of the number of electron-ion pairs below

Table 3 Comparison of WIMP detection techniques

	Threshold	Background	Spectrum Information	Position Information	Additional Signatures	Materials With Spin	Development Status
Proportional Chambers	Few keV	Wire noise? No veto?	Poor	Good	Background Directionality	Yes eg CH ₄	Good Except for noise
Semiconductors	Few keV	Good	Yes	Poor	None	²⁹ Si; ⁷³ Ge	Good
Superconduct. Granules	Few keV?	Poor?	None except by varying threshold	Good	None	Yes	Difficulties: homogeneity of granule sensitivity
Superconduct. with tunnel junctions	?	?	Good	None	None	Yes	Beginning: Reliability of tunnel junctions, trapping
Calorimetry	Few 100eV	Good	Good	Adequate	Ionization?	Yes	Beginning: Parasitic effects in thermistors
Ballistic phonons	?	Good?	Good	Good	Ionization?	Yes	Beginning: Development of sensors

Downloaded from www.annualreviews.org. University of California at Berkeley on 04/12/12. See the Terms and Conditions (http://www.annualreviews.org/terms) on the publisher's website for rules of use; OA articles are governed by the applicable Creative Commons License.

a few keV. Most of the energy is dissipated in excitations, mechanical movements, and eventually heat. This explains why even if the quanta of energy involved in the ionization process (electron-ion pairs in a gas with binding energies of typically 10 eV, electron-hole pairs in semiconductor ionization detectors involving energies of the order of 1 eV) seem small compared to the deposited energies (hundreds of eV), the ionization yield will still be small.

2.3.3.2 Gaseous ionization detectors Proportional chambers are well-developed detectors. In a time projection configuration, the imaging capability may be important for background rejection, as shown by the experience of double β experiments using this type of device (140, 141). At low pressure (e.g. ~ 30 torr) it should be possible to recognize a β of 10 keV from its range (~ 2 cm). As we have mentioned, a recoiling nucleus may also leave a “track” and it may be possible to measure its direction (135). The energy range where this scheme works remains to be experimentally identified. Moreover, this technique faces a number of problems: (a) In spite of the fact that detection of a single electron is technically feasible, the effective threshold may be around a few keV and the resolution will be poor. Thus, proportional chambers may be useful mostly for high m_δ . (b) Another serious problem comes from the background rate in proportional chambers, which without precautions is extremely high (~ 1 count per second and per meter of wire) compared to the required level. It is not clear that radioactivity is the only responsible mechanism. At the level of a few detected electrons, electron extraction from the walls and metastable states may play an important role, and may be more difficult to control. Nothing is known and development is necessary. (c) Finally the need to have several kilograms of gas leads to rather voluminous setups; active veto around the detector may be expensive and impractical.

2.3.3.3 Solid-state ionization detectors Semiconductor ionization detectors suffer from the same problem of low low-energy transfer efficiency to ionization leading to a loss of sensitivity below 10 keV (130). For large germanium detectors of mass 1 kg, the state-of-the-art noise (131) is around 450 eV rms, which, because of the large number of standard deviations (6 or 7) necessary to overcome the noise, leads to ~ 3 keV threshold for electrons. For a recoiling nucleus, which ionizes much less, the effective threshold is ~ 6 keV, too high when $m_\delta < 12 \text{ GeV}/c^2$.

However, these detectors exist and provide the only available limits. Because of the high thresholds, they are currently only useful to reject WIMPs with both large m_δ and large elastic cross sections. Caldwell et al (131) in recent, unpublished work improved the limit of Ahlen et al (133) for a heavy Dirac neutrino, excluding masses down to $12 \text{ GeV}/c^2$.

It is possible to decrease these thresholds with smaller detector elements, which lead to smaller capacitances and electronic noise. The ionization yield typically increases when the atomic number decreases (139), so going to silicon is advantageous. Moreover, for a given m_δ the energy transfer is maximized when the masses of projectile and target nucleus are equal. Thus silicon is a better match for $m_\delta \lesssim 40 \text{ GeV}/c^2$ than is germanium. The combination of these two considerations led the Berkeley–Santa Barbara–Saclay group to propose a silicon detector in order to test the cosmion hypothesis that the solar core is cooled by accreted WIMPs (130). This experiment is being constructed.

More advanced schemes may also be useful. For instance, the use of electron-hole drift in the semiconductor (142) may allow a decrease in the detector element total capacitance and improve the threshold accordingly. A factor of two or three is likely to be within reach (F. Goulding, private communication, March 1988). It may even be possible to have collecting electrodes sufficiently small to allow reliable amplification by avalanche in the semiconductor. At the cost of additional channels, detectors where the electrodes are divided into strips could provide some position resolution, a useful tool to fight the background. A major drawback of this technology is that only two materials can be used, silicon and germanium. It is only in these materials that one can obtain the large region free of carriers (depletion depth) necessary for sizeable detectors of at least several cubic centimeters. Unfortunately these materials are predominantly spinless and it may be necessary to enrich targets in ^{29}Si or ^{73}Ge to be sensitive to Majorana particles. In addition, if the axial charge of neutrons is small, these targets will not be effective (81, 111).

2.3.4 DETECTION METHODS II: CRYOGENIC DETECTORS In an effort to decrease the energy detection threshold, it seems natural to attempt to use quanta of smaller energies than those involved in ionization processes. Cooper pairs in a superconductor have binding energies of the order of 10^{-3} eV , and phonons in a crystal at 100 mK have energies of 10^{-5} eV . If efficient detection schemes using broken Cooper pairs (“quasiparticles”) or phonons can be implemented, the small energy of the quanta involved will lead to very low thresholds. In order to prevent thermal excitation of the quanta from being detected, such detectors have to be maintained at very low temperature, typically much below one Kelvin, and are thus called cryogenic detectors. The potential of such methods for DM searches and other applications has been recognized for some time (143–147).

These detectors can be placed into two main categories: detectors of quasiparticles in a superconducting crystal, and phonon detectors in an insulator. Sadoulet’s review of this (147) contains an extensive list of references.

2.3.4.1 *Quasiparticle detectors* Cooper pairs in a superconductor have binding energies ranging from 4×10^{-5} eV (Ir) to 3×10^{-3} eV (Nb), and the deposition of even a modest amount of energy in a superconductor leads to a large number of broken Cooper pairs (quasiparticles). Two methods have been proposed to detect them.

1. If the detector element is small enough, the superconductivity will be destroyed by the energy deposition. This is the idea behind Superheated Superconducting Granules (148–151). The detector is made of many small spheres a few micrometers in diameter. If they are immersed in a magnetic field, the transition of a single sphere from the superconducting to the normal state can be detected through the suppression of the Meissner effect. The method has been demonstrated but faces a number of technological problems (147 and references therein; 151): manufacturing of regular enough spheres with a uniform sensitivity and a high quantum efficiency, packaging of the spheres to decrease their magnetic interactions, and designing sensitive enough sensors (loops coupled to conventional amplifiers or SQUIDS). Over the last few years, significant progress has been made, and some clever schemes have been suggested such as using the interaction between granules to trigger avalanches and thereby get amplification. But although the method has advantages in other experimental situations (position resolution, large stopping power, built-in memory), it may lack the desired redundancy for DM searches: (a) Close to threshold, where only one ball flips, it is basically a yes-no detector; but we have seen that spectrum information is important to understand the signal and reject the background (e.g. x-ray lines). (b) Because of variation of the grain sensitivity, the threshold may not be very well determined. (c) The present state of the art, where a large proportion of the grains are insensitive, has to be improved considerably before we can reject background based on the fact that only a single grain flipped. (d) The fact that even in that case α particles of ~ 5 MeV basically give the same signal as a low energy event (1 sphere flip) is worrying.

Variations of the above method using superconducting films have been suggested (152–154). They may allow the use of well-developed lithographic techniques to solve the problems with the superconducting grain approach of grain size and position variability, and it may be possible to obtain a roughly linear response (153) for high enough energy deposition. Superconducting wires or filaments (153a) are another possibility.

2. A potentially much more sensitive and accurate method of detecting quasiparticles is to make them tunnel through an insulating barrier between two superconductors (SIS junctions). This method has been studied for some time (155–157). Very encouraging results were recently obtained by Twerenbold & Zehnder at SIN (158, 159) and the von Felitzch

group in Munich (160). Although photolithographic techniques may be used very effectively, outstanding problems still have to be solved in the manufacture of low leakage and sturdy junctions. Many junctions have a poorly understood leakage current in addition to the normal tunnelling of thermally excited quasiparticles (which disappears exponentially when the temperature is lowered). The junctions should also withstand many cool-downs. Making good junctions remains to a large extent “black magic.” The collection of quasiparticles in a large volume is another property important for DM searches. Devices combining a sizeable volume (e.g. 1 cm³) with a small junction (50 × 50 μm) would be very slow. Increasing the size of the junction (to 1 cm²) leads to an unacceptable increase of the noise due to the leakage current. A promising solution based on trapping of quasiparticles in a smaller gap superconductor has been proposed (161), but experimental tests of the idea are just starting.

2.3.4.2 Phonon detectors We now turn to the detection of phonons, which represent even smaller quanta of energy (162, 163). One of the oldest methods for detecting energy is calorimetry, where the absorbed energy ΔE results in a measurable temperature rise

$$\Delta T = \Delta E/C, \quad 10.$$

where C is the heat capacity. If this is done at low enough temperature for C to be very small, the method can in principle be very sensitive and will be able to detect individual particles (144, 162, 163). In practice, a small thermistor is fixed to or implanted in a high-quality crystal that acts as an absorber; its resistance gives the temperature. This is a detector of thermalized phonons and, because of their discrete nature, the detector will experience thermal energy fluctuations. Standard optimum filtering methods (164) taking into account the Johnson noise in the thermistor give a statistical uncertainty in the energy

$$\delta E = \xi(kT^2C)^{1/2}, \quad 11.$$

where ξ depends on the responsivity dR/dT of the thermistor. At temperatures above 100 mK the best thermistors investigated so far are doped semiconductors leading to $\xi \approx 2$. This thermal limit has nearly been achieved by McCammon et al (297) for a small crystal of 10⁻⁵ g of Si. Because of the attachments and the implantation, the total heat capacity of the crystal was roughly equivalent to that of 10⁻⁴ g of Si. The baseline energy fluctuation at 100 mK was measured to be 4.5 eV rms, a very impressive result.

Equation 11 indicates the obvious route for extrapolation to larger

devices (144, 163). Since C is proportional to the mass, and for an insulator C is proportional to $(T/T_D)^3$, where T_D is the Debye temperature,

$$\delta E \sim \xi T^{5/2} M^{1/2} \quad 12.$$

and a large augmentation in mass can in principle be compensated by a modest decrease in temperature. Extrapolating from the results obtained by McCammon and coworkers, it should be possible, if the thermistor resistivity is maintained at low temperature, to get at 15 mK less than 10 eV rms noise for crystals of 320 g of boron, 200 g of silicon, 100 g of germanium! A temperature of 15 mK is relatively easily obtained by modern dilution refrigerators, and cooling down a few kilograms of material is technically feasible. This line of thought has led many groups to develop bolometric detectors.

However, in order to measure the thermistor resistance, it is necessary to put a biasing current through it. It is unfortunately the experience of many groups that, as the temperature decreases, parasitic effects in semiconductors limit the magnitude of this current: a very small current dramatically decreases the resistance of the device and therefore its sensitivity. In spite of recent progress (165, 166) there are still significant problems in enlarging calorimeters operated at low temperature.

It should be noted, however, that the picture outlined above is probably fundamentally incorrect. At low temperature, the absence of thermal phonons will prevent phonons originating from the WIMP interaction from thermalizing efficiently, and the energy of a significant number of them is expected to stay relatively high, around a few meV (167, 168). Such phonons will be ballistic, that is travel in straight lines and bounce off surfaces, and the concepts of temperature and heat capacity are inadequate to describe such a system. These effects are well known to solid-state physicists for large energy depositions, and have recently been demonstrated unambiguously in the context of particle detection (169).

Ballistic phonons may ease the detection job. Instead of the heat capacity of the entire crystal, what counts now is the efficiency of energy collection. The crystal acts as a phonon guide. Because of their fast propagation, the ballistic phonons may allow timing on several faces of the crystal. This requires a fast rise time of the sensor signal. In addition, the fact that energy propagates in preferred directions (“focussing”) may allow the localization of the event within one millimeter by pulse division between several sensors (168).

These ideas are quite attractive, especially in the context of DM detectors where large volumes are necessary. However, it remains to be proven that such detectors can be implemented. Two kinds of sensor are being studied, highly doped semiconductor thermistors, which should be sensitive to

high-energy phonons (166), and superconducting film and tunnel junctions (168). An interesting variant of this method has been suggested for liquid ^4He (170): interactions of high-energy particles lead to the formation of rotons, a special phonon configuration, which can be detected at the surface of the liquid where they eject helium atoms. A silicon bolometer covering the surface will be sensitive to these atoms, which release heat when they are adsorbed on the silicon surface. The great strength of this concept is that liquid helium is extremely pure. However, the method does not provide any spatial resolution, and it remains to be seen if it has the low thresholds and the redundancy necessary for the detection of DM. Also, ^4He will not scatter Majorana fermions.

2.3.4.3 Simultaneous measurement of ionization and heat The simultaneous detection of the ionization and phonon components allow one in principle to give an unambiguous signature for an elastic scattering by a nucleus (144, 171). In that case the ratio of the ionization energy to the total energy released will be 2 to 4 times smaller than for an electron interaction involving the same deposited energy, and only a rough measurement of the ionization yield may be necessary. This attractive method requires the combination of two difficult techniques at very low temperature, and no experimental test has been attempted yet. In addition to silicon and germanium, nonpolar solids such as crystallized hydrogen or noble gases could be used, including liquid helium (171a).

2.3.5 CONCLUSION When designing an experiment, the experimentalist is guided by four criteria (see Table 3):

1. Sensitivity: threshold and irreducible background level should be low enough.
2. Redundancy is necessary to establish the signal and reject spurious backgrounds.
3. The possibility of using a suitable target material should be considered, either matching the projectile mass in a threshold-limited situation, or else maximizing the coupling for Majorana particles by choosing a target with nuclear spin. For instance, boron appears to be an interesting material (171) for light photinos. Because of uncertainties in the spin structure of nuclei and nucleons (see Section 2.2.1), it would be wise to consider a variety of nuclei. Targets where the spin is carried by neutrons and by protons should both be available.
4. State of development: proportional counters and semiconductor ionization detectors exist now, while cryogenic detectors will undoubtedly face a long development.

In the short run, it is likely that the main physics results will be obtained

through improvement in the threshold of “conventional” solid-state detectors.

For large m_ν , low-pressure proportional chambers may become an important experimental tool, if they can be shown to be able to detect a few electrons without spurious noise and to provide directionality and γ -ray background rejection. However, they will be rather bulky and require a large number of channels.

In the long run, if they can be made to work for large masses, cryogenic detectors will become the instruments of choice because of the low thresholds, the variety of materials they should allow, and, perhaps, the signature of a nuclear interaction. However, these detectors face a long development period because of the complexity of the solid-state physics and materials technology that has to be mastered, and the inconvenience of ultra-low-temperature refrigerators.

2.4 *Indirect Detection by Annihilation*

There have been many theoretical suggestions for inferring the existence of dark matter through the observation of annihilation products. So far, no experiment has seen a positive signal. However, sensitivities are approaching the point where useful limits may be placed on the abundance and properties of different types of dark matter. In general, annihilation signals may be avoided by considering WIMPs that possess a cosmological asymmetry; see Table 2 and Section 2.2.1. While it is usually assumed that signals are caused by DM annihilation, we note that similar arguments may be used to constrain decay rates of long-lived but unstable DM candidates.

2.4.1 CAPTURE AND ANNIHILATION IN THE SUN Press & Spergel (73) postulated that WIMPs could be captured by the Sun via elastic WIMP-nucleus scattering. Silk, Olive & Srednicki (172) then showed that the abundance of WIMPs would build to the point where equilibrium would be reached between capture and annihilation. The high-energy neutrinos resulting from those annihilations should be detectable in deep underground proton-decay experiments. Many authors have subsequently contributed to the details of these calculations (80, 126, 173–177), and a variety of underground detectors are starting to collect a significant data sample.

The signal rate depends on the flux of neutrinos produced and the efficiency with which they are detected. In turn, the flux depends on the capture rate of WIMPs by the Sun and the yield of high-energy neutrinos per annihilation; while the detection efficiency depends upon the details of the detector and the signal sought. Two distinct signals have been considered. For “contained” events, a high-energy collision between a

neutrino and a nucleus occurs within the detector. Both charged and neutral current events may occur, but the rate for charged currents dominates by about a factor of three, and are identifiable by the outgoing charged lepton. In principle, the incoming neutrino may be of any type, but in practice the detection rate for tau neutrinos is kinematically suppressed by the tau mass, until neutrino energies are above ~ 20 GeV (173).³ In “throughgoing” events, a muon neutrino undergoes a charged current interaction with a nucleus in the rock (or water) outside the detector (178) and passes the resulting muon through the detector before it stops. These events do not occur for electron neutrinos (the electrons stop too quickly) or for tau neutrinos (the taus decay). The rates expected for these two event types are (126, 173)

$$R_C = 7.2 \times 10 \rho_{.3} \langle v_{300}^{-1} \rangle \sum_N X_N \sigma_{\delta N 38} F_N(m_\delta) \sum_f \Gamma_f \langle N z \rangle_f \text{ kt}^{-1} \text{ yr}^{-1} \quad 13.$$

$$R_T = 7.7 \rho_{.3} \langle v_{300}^{-1} \rangle m_\delta \sum_N X_N \sigma_{\delta N 38} F_N(m_\delta) \sum_f \Gamma_f \langle N z^2 \rangle_f A_6^{-1} \text{ yr}^{-1} \quad 14.$$

where the sum is over nuclear species N ; $\sigma_{\delta N 38}$, $\rho_{.3}$, and v_{300} are defined in Section 2.2; and X_N is the solar abundance of the nuclear species normalized to hydrogen. The function $F_N(m_\delta)$ expresses the kinematic efficiency for capture (119). For Majorana WIMPs, capture in the Sun is dominated by scattering from hydrogen, in which case we may approximate $F_H \approx [m_c^a / (m_c^a + m_\delta^a)]^{1/a}$, with $a = 1.5$ and $m_c = 20.4 m_p$ (126). For WIMPs with vector couplings, capture off other elements may be important (80, 119, 173, 174). For contained events the rate is given per kiloton of detector, while for throughgoing events we scale to A_6 , an area of 10^6 cm². The rates in Equations 13 and 14 assume an isospin neutral detector and equal yields for v 's and \bar{v} 's. The rate R_C for contained events includes ν_e and ν_μ charged current interactions but ignores neutral currents and ν_τ .

The parameters Γ_f are the branching ratios for annihilation into light fermion f and its antiparticle. For contained events the neutrino-nucleon cross section increases linearly with energy so the effective neutrino yield per annihilation into fermion species f is $m_\delta \langle N, z \rangle_f$, where $z = E_\nu / m_\delta$ is the scaled neutrino energy. For throughgoing events, the range of the muon also scales roughly linearly with energy, so the effective neutrino yield scales as z^2 . In Equations 13 and 14, the only fermions that contribute are direct ν production, τ leptons, and c , b , or possibly t quarks. The light quarks and charged leptons are long lived and will come to rest in the core of the Sun before they have a chance to decay weakly and produce a

³ If neutral currents are observable and τ neutrinos dominate the flux, then neutral current ν_τ events may give a bigger signal than that in Equation 13. This may happen for $\bar{\nu}$ models.

neutrino. Yields for the two event types have been estimated using an e^+e^- Monte Carlo to simulate the final states of annihilation events, and are given in Table 4 (126). If one takes detector thresholds and efficiencies into account, the effective yields will be smaller (176). For non-Majorana WIMPs that annihilate through an intermediate Z the yields are dominated by direct ν 's. Majorana WIMPs will not annihilate to neutrinos, because the branching ratios are proportional to m_f^2 .

The signal rates in Equations 13 and 14 are very low. Given the elastic cross sections in Table 2 and the yields in Table 4, we may optimistically expect only a few events per kiloton-year. Fortunately, the backgrounds are also very low. The main source of background is ν 's produced in cosmic-ray air showers (179). The background rate depends on the specific signal. For example, if the final lepton energy is above some threshold E_T (in GeV), the contained event background is $\sim (3/E_T) \text{ kt}^{-1} \text{ yr}^{-1} \text{ sr}^{-1}$ (80). For throughgoing events the background is $\sim 6A_6^{-1} \text{ yr}^{-1}$ (178). Depending upon the energy and angular resolution, the backgrounds may be smaller than the signal. Note that for throughgoing events there is intrinsic angular uncertainty due to the transverse momentum of the muon.

A caveat to the question of annihilation in the Sun is whether or not the WIMPs evaporate from the Sun (80, 104). If the time scale for evaporation is shorter than the time scale to reach equilibrium between annihilation and capture, then the annihilation signal will be suppressed. Evaporation is dominated by a Boltzmann factor $\exp(m_s\phi/T)$, where ϕ and T are the gravitational potential and temperature at the core of the Sun. For the Sun, ϕ and T are fairly well known and the evaporation mass is $m_{ev} \sim 3.0$ GeV, with only a weak dependence upon cross sections, solar abundances, etc.

Three underground detectors [IMB (180), Frejus (181), and Kamioka

Table 4 Neutrino yields from WIMP annihilation in the Sun^a

f	$\langle Nz \rangle \times 10^2$	$\langle Nz^2 \rangle \times 10^2$
τ	5.1	2.30
c	1.2	0.28
b	2.8	0.64
t	5.0	1.55

^a Effective ν_μ yields for contained events, $\langle Nz \rangle$, and throughgoing events, $\langle Nz^2 \rangle$, for annihilation into fermion f. [$m_t = 40$ GeV was assumed (126).] The quantity $z = E_\nu/m_\phi$ is the scaled neutrino energy.

(182)] have reported data on high-energy neutrinos from the Sun. There is no indication of a WIMP annihilation signal in any of the detectors. This information apparently rules out electron and muon sneutrinos as DM candidates (173, 174), unless $m_\delta < m_{\nu_e}$. Other DM candidates have significantly lower neutrino yields than sneutrinos and/or smaller capture rates, so current constraints are only marginally significant. As an example of what may be achieved for $\tilde{\gamma}$'s we show Figure 4 (176), where the data from the Frejus (181) detector has been used to constrain the local halo density in $\tilde{\gamma}$'s as a function of $m_{\tilde{\gamma}}$ for two different models under different assumptions about $\sigma_{\delta p}$. The first feature to notice is that model dependency leads to at least a factor of 5 uncertainty. Second, except for a small range around $m_{\tilde{\gamma}} = 5$ GeV, there are no useful constraints. In fact, because of the low backgrounds reported, the data from all three detectors may be combined (175) to improve the constraint by a factor of 2 from that shown in Figure 4.

Despite the low event rates and current lack of data, prospects for the future are brighter. Experiments an order of magnitude larger are being

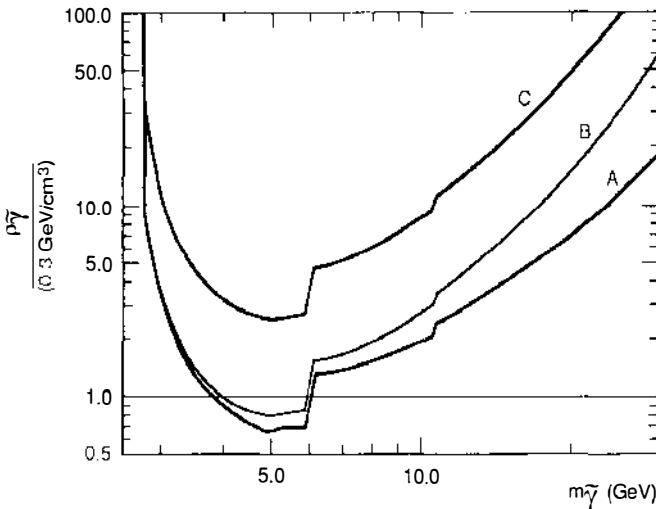


Figure 4 Constraints from nonobservation of high-energy ν 's from photino annihilation in the Sun (adapted from 176). The curves give upper limits to the local $\tilde{\gamma}$ density in units of 0.3 GeV cm^{-3} , assuming that model parameters are adjusted to give $\Omega_{\tilde{\gamma}} h^2 = 0.25$. Curve *A* is for a model with equal squark and slepton masses, and $\sigma_{\delta p}$ determined using the naive quark model. Curves *B* and *C* are for a “minimal supergravity” model, which generically has large squark masses. Curve *B* uses the naive quark model while curve *C* uses $\sigma_{\delta p}$ derived from the EMC experiment. The constraints were derived using neutrino data from the Frejus detector (181). A 2-GeV threshold on neutrino energy accounts for the rise in the limit curves at low $m_{\tilde{\gamma}}$. The “feature” at ~ 6 GeV is associated with details of δ -freezeout at the QCD phase transition.

built. By the early 1990s, roughly 50 kt of detector may be operational—MACRO (~ 20 kt) (183), LVD (~ 12 kt) (184), SuperKamioka (~ 22 kt) (185)—although their efficiency for detecting high-energy solar neutrinos has not been calculated. In addition, there are proposals to construct very large area ($> 10^8$ cm²) detectors—GRAND (186), LENA (187), HLD (188).

Annihilation to ν 's is typically a signal, not background, limited experiment. If we assume hydrogen dominates capture and hold Ω_δ fixed, then $\sigma_{\delta N} \sim m_\delta^{-2}$. In addition, $F_H(m_\delta) \sim m_\delta^{-1}$ above 20 GeV, but above 20 GeV it is typically the throughgoing signal that dominates, and R_T contains an extra factor of m_δ . Thus we find that the signal scales as $S_\nu \sim m_\delta^{-2}$. If background does become a problem it should fall off as m_δ^{-1} for R_C , if appropriate energy cuts are made. The R_T background also decreases roughly as m_δ^{-1} as a result of improved intrinsic angular resolution of the charge exchange vertex.

2.4.2 CAPTURE AND ANNIHILATION IN THE EARTH It is also possible for WIMP capture and annihilation to occur in the Earth, thus producing an observable neutrino flux (122, 189). Considering factors such as mass, distance, and capture efficiency of the Earth (120b) as compared to the Sun, one finds that for WIMPs with vector couplings the Earth gives the better signal, while for Majorana WIMPs the Sun dominates. A key factor is that the Earth is made mostly of heavy elements with zero nuclear spin, which are ineffective in scattering Majorana particles. Even when the WIMPs have vector couplings, the Earth annihilation signal may not be important because the WIMP evaporation mass for the Earth is in the range of $9 < m_{ev} < 13$ GeV [the uncertainty lies in our knowledge of the Earth's core temperature (190)]. Also, WIMPs with vector couplings may possess a cosmological asymmetry, which would preclude an annihilation signal.

2.4.3 GAMMA RAYS FROM ANNIHILATION IN THE GALAXY In the previous two sections we addressed the prospects for detecting annihilation of WIMPs from nearby concentrations in the Sun or the Earth. Here, and in the next two sections, we discuss another “nearby” site for annihilations, our Milky Way Galaxy. The first signal that we discuss is that of high-energy γ rays (124, 125, 191, 192).

Along a given line of sight, the differential flux of high-energy γ 's from WIMP annihilation is

$$\frac{d\Phi}{d\Omega dE_\gamma} = \frac{1}{4\pi} \int \Gamma \frac{dN}{dE_\gamma} dr, \tag{15}$$

Annu. Rev. Nucl. Part. Sci. 1988.38:751-807. Downloaded from www.annualreviews.org by University of California - Santa Cruz on 04/18/12. For personal use only.

where the local annihilation rate per unit volume is $\Gamma = n_\delta^2 \langle \sigma v \rangle_A$ and the differential yield of photons per annihilation event is dN/dE_γ . At low-velocity dispersions we may take $\langle \sigma v \rangle_A$ to be constant, so the flux is just proportional to $\int (\rho^2/m_\delta^2) dr$. For the spherical halo described in Section 2.2.2 this leads to a signal (191, 193)

$$\frac{d\Phi}{d\Omega dE_\gamma} = 3.7 \times 10^{-6} \frac{\langle \sigma v \rangle_{A26}}{m_\delta^2} \rho_{1.0a_{5.6}} F(b, l) \frac{dN}{dE_\gamma} \text{cm}^{-2} \text{s}^{-1} \text{sr}^{-1}, \quad 16.$$

where we have scaled $\langle \sigma v \rangle_A$ to $10^{-26} \text{cm}^3 \text{s}^{-1}$ and expressed m_δ in GeV. The halo parameters ρ_0 and a are scaled to the values in Equations 5. The function $F(b, l)$ (b = galactic latitude, l = galactic longitude) depends upon the line of sight through the halo. For the halo of Equation 4, $F_C + F_A = 2\pi$, where F_C (F_A) are for lines of sight toward the center (anticenter) of our Galaxy. For the parameters of Equation 5, $F_C = 6.02$, $F_A = 0.26$. $F(b, l)$ may plausibly vary by as much as a factor of 2 for nonspherical halos or halos with different core radii (193).

Two proposals have been made for the useful yield of photons. The bulk of the photons are expected to come from π^0 decay, where the neutral pions are produced in the hadronic jets resulting when WIMPs annihilate into a quark-antiquark pair. One may approximate the π^0 production by its value in e^+e^- annihilation at the same center-of-mass energy. Typical yields per annihilation event for 10-GeV WIMPs would be ~ 20 photons carrying $\sim 25\%$ of the total energy, with a spectrum that drops exponentially above a few hundred MeV (125, 194). In addition, annihilation might take place into a bound state of quark-antiquark and a monoenergetic photon (195) with a branching ratio (196) $\sim 2 \times 10^{-4} m_q^2 m_\delta^{-2}$.

For $E_\gamma \gtrsim 100$ MeV the signal in Equation 16 must be detected against a background arising primarily from cosmic-ray interactions in the Galaxy, $\sim 3 \times 10^{-6} (E/\text{GeV})^{-1.5} (\sin b)^{-1} \text{cm}^{-2} \text{s}^{-1} \text{sr}^{-1} \text{GeV}^{-1}$. However, the background is only measured up to 200 MeV by SAS-2 (197),⁴ and theoretical expectations are that the spectrum steepens above a few hundred MeV (200a). Given the different spectral shapes for background and signal, the place to look for the π^0 decays is probably at an E_γ of approximately a few hundred MeV. The latitude dependences of the signal and background are also different, and thus might be used as a discriminant to enhance the signal. However, the observed γ flux is very patchy, with

⁴ The COS-B satellite (198) had larger data samples and reported data in three energy bins, the highest being 0.3–5 GeV. However, it did not look at high latitude, and interpretation is difficult because of high instrumental backgrounds. Refs. (199, 200) are useful monographs on γ -ray astronomy.

variations of ~ 1 from one line of sight to another (197, 198). Averaging over extended regions may help, as would a detailed model for the cosmic-ray-induced background. Another possibility would be to look along lines of sight where the observed flux is fortuitously low and use these to set constraints on WIMP annihilation in the halo. Given the estimate for the branching ratio, in order for the signal-to-background ratio for the line spectrum to be better than that for the π^0 decays the energy resolution of the detector must be $\lesssim 1\%$ (196). However, the line spectrum would be a unique signature, whereas the π^0 decays may be confused with ordinary cosmic-ray physics.

It has been suggested that in addition to its presence in the halo some DM may be entrained in the disk of the Galaxy or perhaps the central spheroid. If either contained a significant fraction of its mass in DM, then lighter WIMPs could generate an observable signal. For example, the central spheroid would act as a 1° source at the galactic center, which optimistically might generate an integrated flux of $\sim 10^{-3} \text{ cm}^{-2} \text{ s}^{-1}$ (201), which is much greater than that observed (202). However, other models yield fluxes lower by a factor of 10^3 or more (203, 204). The fact that there is no evidence for a spheroid or a disk component to the DM distribution from γ -ray data does not imply constraints on WIMP properties since it is not expected that dissipationless DM should be a significant part of these galactic components.

These ideas may be tested to some extent by the Gamma-Ray Observatory (GRO), which is now supposed to be launched in 1990. The EGRET instrument (area \cdot efficiency \cdot solid angle $\sim 10^3 \text{ cm}^2 \text{ sr}$) should have a sensitivity approximately twenty times that of SAS-2 at high energy (205), and should allow a measurement of the diffuse background up to 1 GeV. Unfortunately, the energy resolution is only 15% FWHM so it is unlikely that lines can be detected with this instrument. Larger instruments with better energy resolution (1%) and sky coverage of $2\pi \text{ sr}$ are being designed to be placed on the space station (e.g. 206).

As m_δ increases, the signal-to-background ratio for γ 's decreases as m_δ^{-2} from the number density in the halo. In addition, if we hold Ω_δ constant, then for Majorana WIMPs there is an additional factor of $m_f^2 m_\delta^{-2}$ due to low-energy suppression of $\langle \sigma v \rangle_A$. Because the appropriate energy window will not change radically with m_δ , the background is not greatly reduced as m_δ increases. For the line spectrum, the branching ratio to quarkonium decreases approximately as m_δ^{-2} , a factor that may be compensated for by the decrease in background at higher energy.

2.4.4 ANTIPROTONS FROM ANNIHILATION IN THE GALACTIC HALO A consequence of WIMP annihilation into quarks is the production of some

proton-antiproton pairs (124, 125, 207, 208). Once produced, a \bar{p} will diffuse through the galactic magnetic fields for a time $\tau_{\text{diff}} \sim 10^7\text{--}10^8$ yr before leaking out of the Galaxy. The shorter time scale is for confinement to the disk (207) and the longer is an estimate of confinement time in the halo (124). Both estimates rely on cosmic-ray propagation models designed to fit the abundances of light elements formed in spallation reactions (209). For confinement in the disk, the \bar{p} 's traverse a net distance of only a few hundred parsecs and, therefore, the local \bar{p} flux is set by the local annihilation rate. The differential flux of \bar{p} 's is then

$$\frac{d\Phi}{dE_{\bar{p}}} = 2.2 \times 10^{-3} \frac{\rho_{.3}^2 \langle \sigma v \rangle_{A26}}{m_{\delta}^2} \tau_{15} \beta_{\bar{p}} \frac{dN}{dE_{\bar{p}}} \text{cm}^{-2} \text{s}^{-1} \text{sr}^{-1}, \quad 17.$$

where $\langle \sigma v \rangle_{A26}$ and $\rho_{.3}$ are defined in Section 2.2, m_{δ} is in GeV, and we define $\tau_{15} \equiv \tau_{\text{diff}}/10^{15}$ s. The differential yield of antiprotons $dN/dE_{\bar{p}}$ may be estimated from e^+e^- data (125). Equation 17 implicitly assumes that the energy of the antiproton does not change after it is produced, and that the leakage rate from the Galaxy is energy independent. In fact, it is expected that the spectrum will be modified significantly by the solar wind at low energies (210).

The primary source of background should be \bar{p} 's that result from energetic cosmic-ray interactions in the disk of the Galaxy. However, the models are in disagreement with the data in the energy range 5–10 GeV (211). Although an early experiment indicated otherwise (212), the low-energy data ($T_{\bar{p}} \lesssim 1$ GeV) are not inconsistent with theory (213). An anomaly at low energies would be suggestive of DM annihilation since the kinematics of cosmic-ray interactions make it difficult to produce low-energy \bar{p} 's. Such an event corresponds to a very energetic \bar{p} in the rest frame of the collision, whereas such \bar{p} 's are suppressed by the dynamics of QCD fragmentation. The annihilation signal, on the other hand, is naturally peaked at low energy. Therefore, the maximum signal-to-background ratio is achieved at low kinetic energies $T_{\bar{p}} \lesssim 1$ GeV.

Ahlen et al (213) did not detect any antiprotons with kinetic energy below 1 GeV. This information is not strong enough to place serious constraints on WIMP candidates given realistic halo characteristics (194). A 15-GeV \tilde{h} model proposed (125) to explain the earlier data (212) assumed optimistic values for the halo parameters, cross sections, and yields in Equation 17. With more realistic values, the model is not in conflict with a lack of signal.

For low-energy \bar{p} 's the signal has the same scaling properties with m_{δ} as for the γ -ray signal; specifically, $S_{\bar{p}} \sim m_{\delta}^{-4}$ for Majorana fermions. For antiprotons, the yield and background are both nearly independent of m_{δ} above the threshold for \bar{p} production.

2.4.5 POSITRONS FROM ANNIHILATION IN THE GALAXY Perhaps the least promising signal for galactic annihilations is a positron flux above expectations (124, 125). A major problem with this signal compared to the \bar{p} signal is that the e^+ spectrum will be severely altered as the positrons traverse the Galaxy. Energy loss can occur via Compton scattering or synchrotron radiation. The background is positrons produced in hadronic cosmic-ray interactions, this time from $\pi \rightarrow \mu \rightarrow e$ decays. Because the π 's may be low in energy, and also because of the energy loss mechanisms, there is no clean low-energy signature as exists for \bar{p} 's. A high-energy cutoff at $E_{e^+} = m_\delta$ will be hard to observe because of energy losses and also because the differential yield vanishes smoothly at threshold. If annihilation can occur directly into e^+e^- pairs, then a feature at high energy may be observable (214). This may occur for Dirac neutrinos but not for any Majorana WIMPs.

2.5 *Present Constraints and Future Prospects*

We have discussed several techniques by which a WIMPish DM halo could be detected. In this section, we summarize the current data and compare technologies to see which is most likely to succeed for various WIMP scenarios.

2.5.1 PRESENT CONSTRAINTS Of the techniques discussed in Sections 2.3 and 2.4, only two have provided enough data to say something interesting about WIMPs. Direct detection using ionization technology places constraints on WIMPs that have weak vector couplings to nucleons and $m_\delta \gtrsim 13$ GeV. Trapping DM in the Sun and observing annihilation neutrinos essentially eliminates sneutrinos from consideration. It also achieves some limited success in placing constraints on $\tilde{\nu}$ and \tilde{h} models. Both these technologies stand to improve in the next few years; however, they alone will not suffice to study the full spectrum of possibilities. Unfortunately, none of the other methods we have discussed is mature enough to provide us with useful constraints yet.

2.5.2 SCENARIOS FOR DETECTION We present Table 5 as our estimate of which ideas are most likely to be useful for detecting which WIMPs. We classify the WIMPs by mass and by whether annihilation or asymmetry determines $\Omega_\delta = 1$. In the former category, we consider both vector and axial vector coupling to nuclei. The three mass categories are rather loosely defined. We cut at 3 GeV because this is where the neutrino annihilation signal from the Sun disappears due to evaporation. Also, it is clear that technologies with keV thresholds no longer work for light WIMPs, and so direct detection will rely on the successful development of a cryogenic technology. On the optimistic side, it is for low masses that an annihilation

Table 5 Appropriate experiments for various WIMP scenarios

Motivation for $\Omega_\delta = 1$	Mass		
	$m_\delta \lesssim 3 \text{ GeV}$	$3 \lesssim m_\delta \lesssim 20 \text{ GeV}$	$20 \text{ GeV} \lesssim m_\delta$
Annihilation with vector couplings ^a	C, H	I, ν , H	I, ν
Annihilation with axial couplings	C, H	C, ν , H	ν
Asymmetry	C	I[cosmions]	I

^aI = Direct detection using ionization technology. C = Direct detection using cryogenic technology for low thresholds ($m_\delta \lesssim 3 \text{ GeV}$) or low backgrounds (axial couplings). ν = Indirect detection via neutrinos from the Sun. H = Indirect detection via gammas or antiprotons from the halo. [cosmions] = Solution of the solar neutrino problem requires $4 \leq m_\delta \leq 10 \text{ GeV}$.

signal from the Galaxy is most easily seen. The upper cut at $\sim 20 \text{ GeV}$ reflects the scaling laws discussed in Sections 2.3 and 2.4. For direct detection the signal-to-background ratio gets significantly worse as m_δ increases (unless separation of nuclear recoil and electron recoil events proves feasible). However, for WIMPs with vector couplings to nuclei the event rates should still be large enough for direct detection by ionization to be viable. Signal-to-background ratio also decreases for annihilation signals from the galactic halo. On the other hand, the neutrino signal from annihilations in the Sun is fairly promising. Backgrounds are low and proven technology, albeit expanded to larger scales, can do the job. In the intermediate mass range all experiments have some chance of working when annihilation determines Ω . If asymmetry is a factor, then none of the annihilation signals is expected to be useful. Recall that the cosmion solution to the solar neutrino problem only works if m_δ lies in the range 4–10 GeV.

3. AXIONIC DARK MATTER

3.1 Motivation

The axion is still the most elegant solution to the strong CP problem (215–217). Nonperturbative instanton effects in quantum chromodynamics (QCD) solve the U(1) problem, but violate CP and T . This leads to a neutron electric dipole moment that is nine orders of magnitude larger than the experimental upper limit, unless an otherwise undetermined complex phase $\bar{\theta}$ is arbitrarily chosen to be extremely small. Peccei & Quinn (218) proposed a way to avoid this strong CP problem, by postulating an otherwise unsuspected symmetry (the PQ symmetry) that is spontaneously broken when an associated pseudoscalar field χ_a gets a nonzero vacuum

expectation value $\langle \chi_a \rangle = f_a e^{i\theta}$. The axion (219, 220) is the (pseudo) Goldstone boson associated with this broken symmetry. Nonperturbative QCD effects give the axion a mass $m_a \sim f_\pi m_\pi / f_a$. In the earliest (or “standard”) axion scheme, f_a is associated with the electroweak scale and $m_a \sim 100$ keV. This has now been ruled out by laboratory experiments (215, 216).

The couplings of the axion to matter are proportional to its mass m_a . By introducing a complex scalar boson χ_a with a large vacuum expectation value, the scale of m_a can be decreased so that the axion becomes “invisible.” Two sorts of invisible axion models have been proposed. In one scheme (221, 222) the usual quarks and leptons carry PQ charges. The so-called DFSZ axion mass is related to f_a by

$$\begin{aligned} m_a &= \frac{f_\pi m_\pi}{f_a} \frac{\sqrt{z}}{1+z} N \\ &= 3.7 \times 10^{-5} \text{ eV} (f_a / 10^{12} \text{ GeV})^{-1} (N/6), \end{aligned} \quad 18.$$

where $z = m_u/m_d = 0.55$ according to the standard current algebra analysis and N depends on the PQ charges of the quarks ($N = 6$ is usually assumed). In another (KSVZ or “hadronic” axion) scheme (223, 224), exotic quarks with large masses are the only fermions carrying PQ charges. Both types of axion couple to hadrons and photons via anomalies, but the coupling of the KSVZ axion to leptons is suppressed. The mass of the KSVZ axion is given by Equation 18 with $N = 2$. [We are defining f_a as in (225, 226). Note that some authors (e.g. 227) define f_a twice as large.]

We next summarize the “standard” cosmology of the “invisible” axion, then discuss axion detection, and finally mention several possible complications.

3.2 Cosmological and Astrophysical Constraints

When the temperature in the early universe falls to $T \sim f_a$, the PQ symmetry is broken by $\langle \chi_a \rangle = F_a e^{i\theta}$. The initial value of the phase $\theta_1 = \langle a \rangle / f_a$ is randomly chosen in each causally disconnected region. Later, when the QCD interactions become strong at $T \sim \Lambda_{\text{QCD}} \sim 10^2$ MeV, instanton effects generate a mass for the axion and induce an axion potential that causes θ to oscillate about its minimum-energy value, at which strong CP violation vanishes. This coherent state of axions behaves cosmologically like pressureless dust (i.e. like cold DM) despite the fact that $m_a \ll \Lambda_{\text{QCD}}$ (228).

It is possible to calculate the cosmological energy density Ω_a in these coherent oscillations of the axion field at the present epoch (229–232), and it follows that

$$(f_a/10^{12} \text{ GeV}) \approx 4.3 \times 10^{\pm 0.34} (N/6) F \quad 19.$$

$$m_a/(10^{-5} \text{ eV}) \approx 0.83 \times 10^{\pm 0.34} F^{-1}. \quad 20.$$

The factor F is given by

$$F = (h^2 \Omega_a \gamma \Gamma)^{0.85} (\Lambda_{\text{QCD}}/200 \text{ MeV})^{0.6}, \quad 21.$$

where γ and Γ are factors usually assumed to be of order 1 (discussed below). The requirement $\Omega_a \lesssim 1$ gives an upper bound on f_a and a lower bound on the axion mass and coupling. For $\Omega_a = 0.9$, $h = 1/2$, and $\gamma = \Gamma = \Lambda_{\text{QCD}}/200 \text{ MeV} = 1$, for example, Equation 20 gives $m_a \gtrsim 3 \times 10^{-5} \text{ eV}$.

There are various astrophysical constraints that give lower bounds on f_a , the reasoning behind them all being that, if the axion coupling is too large, axion emission will undermine established astrophysical theories by releasing too much energy (reviewed in 233). Until supernova SN87a, the best constraints on the DFSZ axion were $m_a < 0.01 \text{ eV}$ from He ignition in red giants (234) and $m_a < 0.03 \text{ eV}$ from white dwarf cooling times (235, 236); the best constraint on the KSVZ axion was $m_a < 0.42 \text{ eV}$ from the longevity of helium-burning stars (236, 237). There is also a more direct but less stringent bound on DFSZ axions from nonobservation of axions from the Sun in a germanium detector that utilizes the “axioelectric effect” (enhanced atomic absorption of $\sim \text{keV}$ axion, followed by ejection of an electron): $m_a < 3.7 \text{ eV}$ (238, 239; reviewed in 216). In addition, a proposal has been made to build an axion “helioscope” (240) that would be sensitive to both KSVZ and DFSZ axions for $m_a \gtrsim 1 \text{ eV}$ (241).

There is an interesting new constraint on m_a from the fact that the neutrino signal from SN87a was roughly of the size expected, which implies that neutrinos and not some more exotic species of particle carried away most of the energy. It follows from this that if light particles are more weakly coupled than neutrinos, then they must be much more weakly coupled—since such weakly coupled particles will be emitted by the bulk of the supernova core, while the neutrinos have a mean free path much smaller than the core and are effectively emitted only at the surface of the “neutrino sphere” (242). This strengthens the upper bound on m_a , and the fact that the dominant axion emission process from the supernova, nucleon-nucleon bremsstrahlung (102, 243, 244), is hadronic also makes this bound less sensitive to the model-dependent couplings between axions and leptons.

The resulting bound can be summarized as follows (243):

$$m_a \lesssim 0.75 \times 10^{-3} (T_{\text{core}}/60 \text{ MeV})^{-7/4} \text{ eV}. \quad 22.$$

We emphasize that there is a factor ~ 10 uncertainty in this bound due to

(a) uncertain nuclear physics effects; (b) uncertain supernova physics (such as the core temperature of the supernova, which is probably in the range $30 \lesssim T_{\text{core}} \lesssim 75 \text{ MeV}$); (c) the paucity of ν events actually detected; and (d) details of axion models.

With this upper bound from SN87a and the “standard” axion cosmology, the window of allowed axion masses is remarkably small. Thus if the hypothetical axion exists, it is likely to be important cosmologically, and for $m_a \lesssim 10^{-4} \text{ eV}$ it is gravitationally dominant over baryons.

3.3 *Detection by Conversion to Photons in Laboratory Experiments*

Assuming that axions comprise the dark halo of our galaxy, laboratory experiments might detect them by allowing a tiny fraction of the ambient axions to convert into photons in a precisely tuned microwave cavity (240; reviewed in 5). The coupling of the axion to two photons is proportional to m_a . One of these photons is supplied by the magnetic field B in the cavity, the other is emitted into the cavity with $E_\gamma = m_a c^2 (1 + \frac{1}{2}\beta^2)$, where $\beta \equiv v/c \sim 10^{-3}$ for axions in the halo of our galaxy. For a given local DM density ρ_{DM} in the Galaxy, the number density of axions is inversely proportional to m_a . Thus the power on resonance is proportional to $m_a \rho_{\text{DM}} B^2 V \text{Min}(Q/Q_a, 1)$, where V and Q are the volume and quality factor of the cavity, and $Q_a \approx 2 \times 10^6$ is the “quality factor” of the halo axions (i.e. the ratio of their energy to their energy spread). By making Q high, the axion signal may just be detectable, but at the price of having to search in frequency for several years with many cavities (each tunable by $\sim 10\%$). The results from the first search, at Brookhaven National Laboratory, only ruled out the presence of an axion halo of 300 times the expected density, for axions in a narrow mass range (245). A more sensitive experiment is in preparation at the University of Florida (246).

An alternative axion Compton-like experiment, based on the process $a + e \rightarrow \gamma + e$, has also been proposed (247), using the aligned electron spins in ferrites. But more detailed analyses (248) have shown that such a detector would actually be less sensitive than the microwave cavity detector just described, although alternative schemes might give greater sensitivity.

3.4 *Theoretical Uncertainties*

We have thus far ignored several possible complications, which we now briefly mention. Several physicists (248a) have recently considered mechanisms other than Hubble expansion by which the coherent axion oscillations could dissipate, but none of these work for values of f_a in Equation 19 which give $\Omega_a = 1$. The effect of a possible sudden turn-on of the axion

mass during the QCD phase transition remains uncertain; it may either tighten (249) or weaken (250) the cosmological bound on m_a . Davis (251) argued that axions emitted by oscillating cosmic strings created when the Peccei-Quinn symmetry breaks could contribute two orders of magnitude more energy density than the coherent axion oscillations we have been considering. Although this conclusion was recently challenged (252), more detailed calculations may be necessary to settle the issue.

Two additional sources of uncertainty were included in the factors γ and Γ in Equation 21. Any entropy generated after the temperature falls below T_1 , at which $m_a \approx 3H$, dilutes the axion energy density; γ is defined (232) as the ratio of the entropy per comoving volume now to that when $T = T_1$. This possibility was discussed most recently in (253). Inflation is another issue. We have been implicitly assuming until now that, even if a period of cosmic inflation occurred in the very early universe, the PG phase transition took place after reheating. Equation 20 correspondingly includes an average over the square of the initial axion phase angle θ_1 . But if $T_{\text{reheat}} < T_{\text{PQ}}$, as is likely to be true in inflationary models with small enough fluctuation amplitude to be cosmologically acceptable, then there is no averaging: our entire horizon arose from a region with some particular value of θ_1 , and $\Gamma = 0.17(\theta_1 N/6)^{-2}$ (cf 232, 254–256). Inflation would also avoid the problem of domain walls associated with PQ symmetry breaking (257; reviewed in 216). If θ_1 in our horizon happened to be of order unity, then our previous conclusions are essentially unaffected. But if θ_1 happened to be 10^{-2} and $N = 6$, for example, and we assume $\Omega_a = 0.9$ and $h = 1/2$, then $m_a \lesssim 5 \times 10^{-8}$ eV and axion detection experiments will see nothing.

Finally, it is also possible of course that the strong CP problem is solved without the need for axions, perhaps by soft CP violation (cf 216) or else by $m_u = 0$. [Although this latter possibility is apparently not excluded by the data (258, 259), there seems to be no good reason why any quark mass should exactly vanish.]

Thus, sadly, if an axion detector does not detect axions, there are many possible explanations. On the other hand, Nature could be kind and $m_a \approx 10^{-5}$ eV. It is worth looking.

4. LIGHT NEUTRINOS

The only elementary particle candidates for dark matter that we know actually exist are the light neutrinos (260–263).⁵ For definiteness, we assume that the neutrino chemical potential (266, 267) is negligible.

⁵Other, more speculative possibilities with similar astrophysical properties include a majoron (264, 265), a light photino (100, 101) (no longer favored in supersymmetric models), or a light higgsino (86).

For each light neutrino species “i”, the number density of $\nu_i + \bar{\nu}_i$ at the present era is (79)

$$n_{\nu,0} = \frac{3}{4} \cdot \frac{4}{11} n_{\gamma,0} = 109\theta^3 \text{ cm}^{-3}, \tag{23}$$

where $\theta \equiv (T_0/2.7 \text{ K})$. Since the present cosmological density is $\bar{\rho} = \Omega\rho_c = 11\Omega h^2 \text{ keV cm}^{-3}$, it follows that

$$\sum_i m_{\nu_i} < \bar{\rho}/n_{\nu,0} \leq 100\Omega h^2 \theta^{-3} \text{ eV}, \tag{24}$$

where the sum runs over all stable neutrino species with $m_{\nu_i} \leq 1 \text{ MeV}$. Thus if one species of neutrino dominates the cosmological mass density, then a reasonable estimate for its mass is $m_\nu \sim 25 \text{ eV}$ (assuming, say, $\Omega = 1$ and $h = 0.5$).

At present the only experimental evidence for nonzero neutrino mass, that of the Russian group (268), is not entirely convincing. The other tritium β -decay experiments (269, 270) and the neutrino signal from SN87a (271–275) imply an upper bound of $m_{\nu_e} \lesssim 20 \text{ eV}$, and of course no limits on the masses of other neutrino species. The so far unsuccessful attempts to detect neutrino oscillations give only upper limits on neutrino masses multiplied by (essentially unknown) mixing parameters. Perhaps the best way to measure the masses of ν_μ and ν_τ in the cosmologically interesting range of tens of eV is through the dispersion of the neutrino flux from a galactic supernova, and its subsequent detection via neutral current disassociation of deuterium (276).

“Hot” DM is the theory stating that galaxies and large-scale structures form in the universe by the growth in amplitude and eventual gravitational collapse of fluctuations in which the dominant component is light neutrinos (or similar particles). The crucial feature of hot DM is the erasure of small fluctuations by free streaming. The minimum mass of a surviving fluctuation is of order $M_{\text{Pl}}^3/m_\nu^2 \sim 10^{15} M_\odot$ (277, 278). A more careful calculation (278, 279) gives

$$M = 1.77 M_{\text{Pl}}^3 m_\nu^{-2} = 3.2 \times 10^{15} (m_\nu/30 \text{ eV})^{-2} M_\odot, \tag{25}$$

which is the mass scale of superclusters. Objects of this size are the first to form in a ν -dominated universe, and smaller-scale structures such as galaxies can form only after the initial collapse of supercluster-size fluctuations. However, the weight of evidence suggests that galaxies are much older than superclusters, which are only now beginning to collapse. For this and other reasons, hot DM is generally regarded as less successful than cold DM (e.g. 47, 280).

Neutrinos could be the DM in other theories of structure formation.

For example, in schemes in which the seeds for forming galaxies and clusters are loops of cosmic string, neutrino DM perhaps works better than cold DM (281, 282). It is even conceivable that light neutrinos could be candidates for cold DM (283). However, light neutrinos cannot be the DM in the halos of the smallest galaxies. Both theoretical arguments regarding the dwarf spheroidal (dS) satellite galaxies of the Milky Way (284) and data on Draco, Carina, and Ursa Minor (285, 286) imply that dark matter dominates the gravitational potential of these dS galaxies. But phase-space constraints (287) set a lower limit (286) $m_\nu > 500$ eV, which is completely incompatible with the cosmological constraint in Equation 24. (Note that even if we assume neutrinos are the DM in large spiral galaxies, the phase-space constraint implies $m_\nu \gtrsim 30$ eV). Thus, not all of the DM can be light neutrinos.

It appears that light neutrino DM would be essentially impossible to detect. The forces neutrinos would exert by reflection or refraction are miniscule (288–293). Neutrino decay could conceivably lead to a signal, but the lifetime of a light neutrino is probably too long for this to be detectable (294, 295). Another effect that would probably be impossible to observe is the annihilation of high-energy cosmic-ray neutrinos on DM neutrinos (296).

5. SUMMARY

This is a mid-1988 status report on attempts to detect particle dark matter (DM). We have shown some prejudice in limiting ourselves to DM candidates that we feel are especially well motivated: weakly interacting massive particles (WIMPs), axions, and light neutrinos. Much of our review centers on the possibility of detecting WIMPs. This is partly because there exist several methods by which WIMPs may be detected in the next decade, whereas for axions the prospects are more uncertain and for light neutrinos essentially nonexistent. In addition, we feel that WIMPs provide a natural way for a critical density of DM to occur within the context of plausible particle theories.

We summarized the currently available data and future possibilities for WIMP detection in Section 2.5. The bottom line is optimistic: most WIMP scenarios admit detection of DM via one or more of the techniques discussed in Section 2. Moreover, a large community of physicists is involved in the development work. In contrast, there is essentially only one method currently proposed for detecting a cosmologically interesting density of axions, the prospects are not especially strong for success, and only a small number of physicists are involved. The only way (that we know) to detect a cosmologically interesting μ or τ neutrino mass is via flight-time delays

in the neutrino pulse from a galactic supernova. This would require several sophisticated neutrino detectors to be on line at the right time, a vast investment in capital and patience.

5.1 *Uncertainties*

We feel it is important to stress the uncertainties inherent in DM searches. Although it goes strongly against current wisdom, until we identify the source of the observed gravitational effects we cannot be absolutely sure that DM exists, let alone that it is nonbaryonic. There exists a host of models (that we do not find compelling) in which DM takes an essentially unobservable form. In addition, the properties of the local DM distribution are not known to better than a factor of two. These are generic problems.

For WIMPs there is a special list of problems. Expectations for event rates depend upon a number of uncertain quantities besides the halo density of DM. The cross sections have a number of sources of uncertainty. (a) Cosmological quantities are not known to better than a factor of two, which affects our expectations for the strength of WIMP interactions. (b) More realistic models have a number of unknown parameters that alter predictions. (c) There is unknown nuclear and particle physics that may change the elastic WIMP-nucleus cross sections by as much as an order of magnitude. Further, most of the proposed detection schemes have backgrounds that are not fully understood, so the criteria for successful detection are uncertain.

For axions, the chief uncertainty comes from the cosmology of the very early universe. Either the standard model of axion cosmology applies, or it does not. If it does, then considerable effort may result in detection. If it does not, then although axions may account for $\Omega = 1$, they may remain undetectable. Thus, a null result in these experiments does not place severe constraints on either axions or the astrophysics of DM. But success could teach us a great deal about the origin of the universe.

5.2 *What If?*

Identification of the DM is one of the most important tasks confronting physicists and astronomers today. What if we don't succeed? We are still left wondering what the universe is about. We may learn something important about particle physics from nondetection. Unfortunately, it is also quite possible that this negative information will not take us very far. As already mentioned, failure to detect axions may say something no more interesting than that the standard axion cosmology is too naive. For WIMPs, failure to see *any* signal must place *some* constraints on model building, especially for supersymmetric theories. However, we remind the

reader that we have assumed that the DM candidate under consideration is responsible for $\Omega = 1$. It may well turn out that the world is supersymmetric and that there is a light superpartner, but that $\Omega_{\text{LSP}} \ll 1$. In this case failure of WIMP searches says something about model parameters, but may not rule out a wide class of models.

What if we do succeed? Discovering what the universe is mostly made of would doubtless have an important impact on particle theory and cosmology—especially on theories of galaxy formation. Moreover, once DM is identified, our cleverness in detecting and using it will grow. For example, if it turns out that DM consists of WIMPs that undergo annihilation, then the galactic annihilation signals discussed here may prove to be probes of galactic structure, even if they were not instrumental in the original identification.

We hope that at least one of the experiments discussed in this article will have positive results and that the hard work and patience of hundreds of our colleagues will be rewarded.

[Please see Note Added in Proof, page 806.]

ACKNOWLEDGMENTS

The authors have benefitted from discussions with G. Blumenthal, A. Dekel, J. Ellis, S. M. Faber, J. Faulkner, R. Flores, K. Freese, J. Frieman, T. Gaisser, A. Gould, K. Griest, H. Haber, G. Kane, Rocky Kolb, L. Krauss, R. Lanou, R. Mayle, H. Meyer, K. Olive, S. Raby, G. Raffelt, M. Reese, S. Ritz, P. Sikivie, J. Silk, D. Spergel, F. Stecker, M. Srednicki, G. Steigman, L. Stodolsky, G. Tarlé, S. Tilav, M. Turner, T. Walker, G. West, and F. Wilczek. We thank Steven L. Allen for help with Figure 3a; and the Aspen Center for Physics, where we received many useful criticisms.

In addition, B.S. gratefully acknowledges enlightening discussions with N. Booth, B. Cabrera, A. Coron, A. Drukier, F. von Feilitzch, E. Haller, A. Lange, D. McCammon, H. Moseley, B. Neuhauser, T. Niinikoski, K. Pretzl, P. Richards, G. Seidel, E. Silver, G. Waysand, and A. Zehnder, in particular on many solid-state physics and instrumental aspects of the cryogenic detectors. He discussed with many other colleagues potential applications, in particular with D. Caldwell, E. Commins, E. Fiorini, R. Lanou, R. Ross, P. Smith, and H. Steiner.

This work was partially supported by US Department of Energy contract No. DE-AC03-76SF00098 at Berkeley, and NSF grants PHY-8415444 and 8741482 at UCSC.

Literature Cited

1. Faber, S. M., Gallagher, J. S., *Ann. Rev. Astron. Astrophys.* 17: 135 (1979)
2. Trimble, V., *Ann. Rev. Astron. Astrophys.* 25: 425-72 (1987)
3. Kormendy, J., Knapp, G. R., eds., *Dark Matter in the Universe*, I.A.U. Symp. No. 117. Dordrecht: Reidel (1987).
4. Faber, S. M., ed., *Nearly Normal Galaxies*. Berlin: Springer-Verlag (1987).
5. Smith, P. F., In *Cosmology, Astronomy, and Fundamental Physics: 2nd ESO-CERN Symp.*, Eur. Southern Observatory Conf. and Workshop Proc. No. 23, ed. G. Setti, L. van Hove, Garching bei München: ESO (1986), pp. 237-63; Revised version: Smith, P. F., Lewin, J. D., *Rutherford Appleton Lab. preprint RAL-88-045* (1988)
6. Rubin, V. C., *Science* 220: 1339 (1983)
7. van Albada, T. S., Sancisi, R., *Philos. Trans. R. Soc. London A320*: 447-64 (1986)
8. Blumenthal, G., et al., *Nature* 311: 517-25 (1984).
9. White, S. D. M., Rees, M. J., *Mon. Not. R. Astron. Soc.* 183: 341 (1978)
10. Fall, S. M., Efstathiou, G., *Mon. Not. R. Astron. Soc.* 193: 189 (1980)
11. Blumenthal, G., et al., *Astrophys. J.* 301: 27 (1986).
12. Barnes, J., See Ref. 4, pp. 154-59
13. Ryden, B., Gunn, J., *Astrophys. J.* 318: 15-31 (1987)
14. Audouze, J., Szalay, A., eds., *Evolution of Large Scale Structures in the Universe*, I.A.U. Symp. No. 130. Dordrecht: Reidel. In press (1988)
15. Blumenthal, G., See Ref. 14
16. Peebles, P. J. E., *Nature* 321: 27 (1986)
17. Dekel, A., Rees, M. J., *Nature* 326: 455 (1987)
18. Yahil, A., In *Proc. Vatican Study Week on Large-Scale Motions in the Universe*, ed. V. Rubin, G. Coyne. In press (1988)
19. Loh, E. D., Spillar, E. J., *Astrophys. J. Lett.* 307: L1 (1986)
20. Bahcall, S. R., Tremaine, S., *Astrophys. J. Lett.* 326: L1 (1988)
21. Blau, S. K., Guth, A. H., Linde, A. D., In *300 Years of Gravitation*, ed. S. W. Hawking, W. Israel, Cambridge Univ. Press (1987)
22. Turner, M., In *Proc. 17th GIFT Seminar. Cosmology and Particle Physics*, ed. E. Alvarez, et al. Singapore: World Sci. (1987)
23. Banks, T., *Preprint SCIPP88/09*, Univ. Calif. Santa Cruz (1988)
24. Coleman, S., *Preprint, Harvard Univ. HUTP-88/A022* (1988)
25. Vittorio, N., Silk, J., *Astrophys. J. Lett.* 285: L39 (1984)
26. Bond, J. R., Efstathiou, G., *Astrophys. J. Lett.* 285: L45 (1984)
27. Kaiser, N., Silk, J., *Nature*. In press (1988)
28. Vishniac, E., *Astrophys. J.* In press (1988)
29. Bond, J. R., Efstathiou, G., *Mon. Not. R. Astron. Soc.* 227: 33 (1987)
30. Kaiser, N., Lasenby, J., eds. *The Post-Recombination Universe*. In press (1988)
31. Readhead, A., et al., See Ref. 30
32. Boesgaard, A., Steigmen, G., *Ann. Rev. Astron. Astrophys.* 23: 319 (1985)
33. Applegate, J. H., Hogan, C. J., Scherrer, R. J., *Phys. Rev.* 35: 1151 (1987)
34. Alcock, C. R., Fuller, G. M., Mathews, G. J., *Astrophys. J.* 320: 439 (1987)
35. Dimopoulos, S., et al., *Preprint SLAC-PUB-4356*. Stanford, Calif: SLAC (1987)
36. Peebles, P. J. E., *Astrophys. J. Lett.* 315: L73 (1987)
37. Hegyi, D., Olive, K., *Astrophys. J.* 303: 56 (1986)
38. Carr, B. J., Bond, J. R., Arnett, W. D., *Astrophys. J.* 277: 445 (1984)
39. Larson, R. B., *Comments Astrophys.* 11: 273 (1987)
40. Ashman, E. M., Carr, B. J., *Preprint*. London: Queen Mary Coll. (1988)
41. Bahcall, J. N., *Astrophys. J.* 276: 169-81 (1984)
42. Kuijken, K., Gilmore, G., *Nature*. Submitted (1987)
43. Turner, M., See Ref. 3, pp. 445-88
44. Nitz, D., et al., *Univ. Mich. Preprint UM HE 86-16* (1986)
45. Rich, J., Lloyd Owen, D., Spiro, M., *Phys. Rep.* 151: 239 (1987)
46. Dover, C. B., Gaisser, T. K., Steigman, G., *Phys. Rev. Lett.* 42: 1117 (1979)
47. Primack, J. R., In *Proc. Int. Sch. Phys. "Enrico Fermi," Course 92*, ed. N. Cabibbo. Amsterdam: North-Holland, pp. 137-241 (1987)
48. Davis, M., et al., *Astrophys. J.* 292: 371 (1985)
49. Dekel, A., Faber, S. M., Davis, M., In *From the Planck Scale to the Weak Scale: Toward a Theory of the Universe*, Proc. 1986 Theor. Adv. Study Inst. on Elem. Part. Phys., ed. H. Haber. Singapore: World Scientific (1987), pp. 787-943
50. Zel'dovich, Ya. B., *Mon. Not. R. Astron. Soc.* 192: 663 (1980)

51. Kibble, T. W. B., *Phys. Rep.* 67: 183 (1980)
52. Vilenkin, A., *Phys. Rep.* 121: 263 (1985)
53. Turok, N., See Ref. 14
54. Ostriker, J., Cowie, L., *Astrophys. J. Lett.* 243: 127 (1980)
55. Ostriker, J., See Ref. 14
56. Rees, M., *Mon. Not. R. Astron. Soc.* 218: 25 (1986)
57. Fall, S. M., Rees, M. J., *Astrophys. J.* 298: 18 (1985)
58. Blumenthal, G., Rosenblatt, E., Faber, S., *Astrophys. J.* 330: 191 (1988)
59. Dekel, A., Silk, J., *Astrophys. J.* 303: 39 (1986)
60. Rees, M., *Mon. Not. R. Astron. Soc.* 213: 75 (1985)
61. Silk, J., *Astrophys. J.* 297: 1 (1985)
62. Dekel, A., *Comments Astrophys.* 11: 235-56 (1986)
63. Kirschner, R. P., et al., *Astrophys. J.* 248: L47 (1981)
64. White, S. D. M., et al., *Astrophys. J.* 313: 505 (1987)
65. Burstein, D., et al., In *Galaxy Distances and Deviations from Universal Expansion*, ed. B. F. Madore, B. Tully. Dordrecht: Reidel (1986), pp. 123-30
66. Lynden-Bell, D., et al., *Astrophys. J.* 326: 19-49 (1988)
67. Bertschinger, E., See Ref. 30
68. Bahcall, N., Soneira, R., *Astrophys. J.* 277: 27 (1984)
69. Blumenthal, G., Dekel, A., Primack, J., *Astrophys. J.* 326: 539-50 (1988)
70. Steigman, G., et al., *Astron. J.* 83: 1050 (1978)
71. Faulkner, J. Gilliland, R. L., *Astrophys. J.* 299: 994 (1985)
72. Spergel, D. N., Press, W. H., *Astrophys. J.* 294: 663 (1985)
73. Press, W. H., Spergel, D. N., *Astrophys. J.* 296: 679 (1985)
- 73a. Nauenberg, M., *Phys. Rev.* D36: 1080 (1987)
74. Rowley, J. K., et al., In *Solar Neutrinos and Neutrino Astronomy*, ed. M. L. Cherry, et al., AIP Conf. Proc. 126. New York: AIP (1984)
75. Bahcall, J., Ulrich, R., *Rev. Mod. Phys.* 60: 297 (1988)
76. Nakahata, M., *Univ. Tokyo Preprint UT-ICEPP-88-01* (1988)
77. Lee, B. W., Weinberg, S., *Phys. Rev. Lett.* 39: 165 (1977)
78. Hut, P., *Phys. Lett.* 69B: 85 (1977)
79. Steigman, G., *Ann. Rev. Nucl. Part. Sci.* 29: 313 (1979)
80. Griest, K., Seckel, D., *Nucl. Phys.* B283: 681 (1987); B296: 1034 (1988)
81. Goodman, M. W., Witten, E., *Phys. Rev.* D31: 3059 (1986)
82. Kolb, E. W., Olive, K. A., *Phys. Rev.* D33: 1202; D34: 2531 (1986)
83. Pagels, H., Primack, J., *Phys. Rev. Lett.* 48: 223-26 (1982)
84. Primack, J., In *Particles and Fields 2, Proc. 1981 Banff Summer Inst.*, ed. A. Z. Capri, A. N. Kamal. New York: Plenum (1983), pp. 607-19
85. Goldberg, H., *Phys. Rev. Lett.* 50: 1419 (1983)
86. Ellis, J., et al., *Nucl. Phys.* B238: 453 (1984)
87. Hagelin, J. S., Kane, G. L., Raby, S., *Nucl. Phys.* B241: 638 (1984)
88. Ibanez, L. E., *Phys. Lett.* 137B: 160 (1984)
89. Haber, H. E., Kane, G. L., *Phys. Rep.* 117: 75-263 (1985); *Sci. Am.* 254(6): 52 (1986)
90. Witten, E., *Nucl. Phys.* B166: 513 (1981)
91. Farrar, G. R., Fayet, P., *Phys. Lett.* 76B: 575; 79B: 442 (1978)
92. Farrar, G. R., Weinberg, S., *Phys. Rev.* D27: 2732 (1983)
93. Hall, L., Suzuki, M., *Nucl. Phys.* B231: 419 (1984)
94. Lee, I. H., *Nucl. Phys.* B246: 120 (1984)
95. Mohapatra, R., Aulakh, C., *Phys. Lett.* 119B: 136 (1983)
96. Bouquet, A., Salati, P., *Nucl. Phys.* B284: 557 (1987)
97. Blumenthal, G., Pagels, H., Primack, J., *Nature* 299: 37 (1982)
98. Barnett, M., Haber, H., Kane, G., *Nucl. Phys.* B267: 625 (1986)
- 98a. Albajar, C., et al., *Phys. Lett.* 198B: 261 (1987)
99. Burke, D., See Ref. 49, pp. 497-540
100. Cabibbo, N., Farrar, G., Maiani, L., *Phys. Lett.* 105B: 155 (1981)
101. Sciama, D., *Phys. Lett.* 112B: 211; 114: 19; 118: 327 (1982)
102. Raffelt, G., Seckel, D., *Phys. Rev. Lett.* 60: 1793 (1988)
103. Srednicki, M., Olive, K., Silk, J., *Nucl. Phys.* B279: 804 (1987)
104. Gould, A., *Astrophys. J.* 321: 560 (1987)
105. Gilliland, R. L., et al., *Astrophys. J.* 306: 703 (1986)
106. Krauss, L. M., et al., *Astrophys. J.* 299: 1001 (1985)
107. Gelmini, G. B., Hall, L. J., Lin, M. L., *Nucl. Phys.* B281: 726 (1987)
108. Raby, S., West, G., *Phys. Lett.* 194B: 557 (1987); *Nucl. Phys.* B292: 793 (1987); *Phys. Lett.* 200B: 547 (1988)
109. Raby, S., West, G., *Los Alamos Preprint LA-UR-87-3664* (1987)
110. Drukier, A. K., Freese, K., Spergel, D., *Phys. Rev.* D33: 3495 (1986)

111. Ellis, J., Flores, R. A., *Preprint CERN-TH.4911/87*. Geneva: CERN (1987)
112. Kane, G. L., Kani, I., *Nucl. Phys.* B277: 525 (1986)
113. Ashman, J., et al., *Preprint CERN-EP/87-230* Geneva: CERN (1987)
114. Griest, K., *Fermilab Preprint 88/74-A*. Batavia, Ill: Fermi Natl. Accel. Lab. (1988)
115. Kerr, F. J., Lynden-Bell, D., *Mon. Not. R. Astron. Soc.* 221: 1023-38 (1986)
116. Binney, J., Tremaine, S., *Galactic Dynamics*. Princeton Univ. Press, NJ (1987)
- 116a. Ostriker, J. P., Caldwell, J. A. R., *Astrophys. J.* 251: 61 (1981)
- 116b. Bahcall, J. N., Schmidt, M., Soneira, R. M., *Astrophys. J.* 265: 730 (1983)
117. Flores, R. A., *Preprint CERN-TH.4736/87*. Geneva: CERN (1987)
118. Campbell, B. A., et al., *Phys. Lett.* 173B: 270 (1986)
119. Gould, A., *Astrophys. J.* 321: 571 (1987)
120. Griest, K., *Phys. Rev.* D37: 2703 (1988)
- 120a. Freese, K., Frieman, J., Gould, A., *Preprint SLAC-PUB-4427*. Stanford, Calif: SLAC (1988)
- 120b. Gould, A., *Astrophys. J.* 328: 919 (1988)
121. Griest, K., Sadoulet, B., Preprint in preparation (1988)
122. Krauss, L. M., Srednicki, M., Wilczek, F., *Phys. Rev.* D33: 2079 (1986)
123. Oh, K.-S., Blumenthal, G., Primack, J., Preprint in preparation (1988)
124. Silk, J., Srednicki, M., *Phys. Rev. Lett.* 53: 624 (1984)
125. Rudaz, S., Stecker, F. W., *Astrophys. J.* 325: 16 (1988)
126. Ritz, S., Seckel, D., *Nucl. Phys.* B304: 877 (1988)
127. Sjostrand, T., *Lund Univ. Preprint LU TP 85-10* (1985)
128. Wasserman, I., *Phys. Rev.* D33: 2071 (1986)
129. Drukier, A. K., Freese, K., Spergel, D. N., *Phys. Rev.* D33: 3495 (1986)
130. Sadoulet, B., et al., *Astrophys. J. Lett.* 324: L75 (1988)
131. Caldwell, D. O., et al., *Phys. Rev. Lett.* Submitted (1988)
132. Martoff, C. J., *Science* 237: 507 (1987)
133. Ahlen, S. P., et al., *Phys. Lett.* 195B: 603 (1987)
134. Spergel, D., *Phys. Rev. Lett.* D37: 1353 (1988)
135. Rich, J., Spiro, M., *Saclay Preprint DPhPE 88-04* (1988)
136. Deleted in proof
137. Caldwell, D. O., et al., *Phys. Rev. Lett.* 59: 419 (1987)
138. Ellis, J., Flores, R., *CERN Preprint CERN-TH-5040/88*. Geneva: CERN (1988)
139. Lindhard, J., et al., *Kgl. Dan. Vidensk. Selsk., Mat.-Fys. Medd.* 33: 10 (1963)
140. Iqbal, M. A., et al., *Nucl. Instrum. Methods* A243: 459 (1986)
141. Elliott, S. R., et al., *Phys. Rev. Lett.* 56: 2582 (1986)
142. Rehak, P., et al., *Nucl. Instrum. Methods* A248: 367 (1986)
143. Drukier, A. K., Stodolsky, L., *Phys. Rev.* D30: 2295 (1984)
144. Cabrera, B., Krauss, L. M., Wilczek, F., *Phys. Rev. Lett.* 55: 25 (1985)
145. Cabrera, B., Caldwell, D. O., Sadoulet, B., In *Proc. 1986 Summer Study on the Physics of the Superconducting Supercollider*, ed. R. Donaldson, J. Marx. New York: Am. Phys. Soc. (1987), p. 704
146. IEEE Nucl. Sci. Symp., San Francisco (October 1987). *IEEE Trans. Nucl. Sci.* 35 (1988)
147. Sadoulet, B., See Ref. 146, p. 42
148. Bernas, H., et al., *Phys. Lett.* 24A: 721 (1967)
149. Drukier, A. K., et al., *Lett. Nuovo Cimento* 14: 300 (1975)
150. Drukier, A. K., Yuan, L. C. L., *Nucl. Instrum. Methods* 138: 213 (1976)
- 150a. Drukier, A., Freese, K., Frieman, J., *SLAC Preprint Slac-PUB-4497*, submitted to *J. Appl. Phys.* (1988)
151. Pretzl, K., *Preprint Max Planck Institut Munich MPI-PAE/Exp.El.187* (1987)
152. Sherman, N. K., *Can. J. Phys.* 40: 372 (1962)
153. Neuhauser, B., et al., In *Proc. 18th Int. Conf. on Low Temperature Physics, Kyoto, Jpn. J. Appl. Phys.* 26: (1987)
- 153a. Smith, P. F., *Z. Phys.* C31: 265 (1986)
154. Neuhauser, B., et al., See Ref. 146, p. 65
155. Wood, G. H., White, B. L., *Appl. Phys. Lett.* 15: 237 (1969)
156. Kurakado, M., Mazaki, H., *Phys. Rev.* D22: 168 (1980)
157. Barone, A., de Stefano, S., Gray, K. E., *Nucl. Instrum. Methods* A235: 254 (1985)
158. Twerenbold, D., *Europhys. Lett.* 1: 209 (1986)
159. Twerenbold, D., Zehnder, A., *J. Appl. Phys.* 61: 1 (1987)
160. Krauss, H., et al., *Europhys. Lett.* 1: 161 (1986)
161. Booth, N. E., *Appl. Phys. Lett.* 50: 293 (1987)
162. Niinikoski, T. O., Udo, F., *CERN NP Rep. 74-6*. Geneva: CERN (1974)
163. Fiorini, E., Niinikoski, T. O., *Nucl. Instrum. Methods* 224: 83-88 (1984)
164. Moseley, S. H., Mather, J. C., McCammon, D., *J. Appl. Phys.* 56(5): 1257 (1984)

165. Moseley, S. H., et al., See Ref. 146, p. 59
166. Wang, N., et al., See Ref. 146, p. 55
167. Maris, H. J., In *5th Int. Conf. on Phonton Scattering in Condensed Matter*, Urbana, Illinois, June 2-6, 1986. Preprint COO-3130TC-29 (1986)
168. Neuhauser, B., et al., 1986 *Applied Superconductivity Conf.*, Baltimore (1986)
169. Peterreins, Th., et al., See Ref. 146, p. 70
170. Lanou, R. E., Maris, H. J., Seidel, G. M., In *Proc. Workshop on Low Temperature Detectors for Neutrinos and Dark Matter*, ed. K. Pretzl., N. Schmidt, L. Stodolsky. Berlin, Heidelberg: Springer-Verlag (1987), p. 150
171. Sadoulet, B., In *Proc. 13th Texas Symp. on Relativistic Astrophysics*, ed. M. L. Ulmer. Singapore: World Sci. (1987), p. 260
- 171a. Lanou, R. E., Maris, H. J., Seidel, G. M., In *23rd Rencontre de Moriond Workshop on Dark Matter* (1988)
172. Silk, J., Olive, K., Srednicki, M., *Phys. Rev. Lett.* 55: 257 (1985)
173. Gaisser, T. K., Steigman, G., Tilav, S. Z., *Phys. Rev. D*34: 2206 (1986)
174. Ng, K., Olive, K. A., Srednicki, M., *Phys. Lett.* 188B: 138 (1987)
175. Olive, K., Srednicki, M., *Preprint Univ. Minn. UMN-TH-636/87* (1987)
176. Ellis, J., Flores, R. A., Ritz, S., *Phys. Lett.* 198B: 393 (1987)
177. Hagelin, J. S., Ng, K., Olive, K., *Phys. Lett.* 180B: 375 (1987)
178. Gaisser, T. K., Stanev, T., *Phys. Rev. D*30: 985 (1984); *D*31: 2770 (1985)
179. Perkins, D. H., *Ann. Rev. Nucl. Part. Sci.* 34: 1 (1984)
180. Losecco, J. M., et al., *Phys. Lett.* 188B: 388 (1987)
181. Frejus Collaboration, presented by B. Kuznik, *Orsay Preprint LAL-87-21* (1987)
182. Totsuka, Y., *Univ. Tokyo Preprint UT-ICEPP-87-02* (1987)
183. MACRO Collaboration, *Nucl. Instrum. Methods A*264: 18 (1988)
184. Bari, C., et al., *Nucl. Instrum. Methods A*264: 5 (1988)
185. Totsuka, Y., *7th Workshop on Grand Unification, ICOBAN '86* Toyama, Japan (1986)
186. Ellsworth, R., et al., *Univ. Calif. Irvine Neut No. 87-38* (1987)
187. Koshihina, M., Presented at Extra Solar Neutrino Workshop, UCLA (Oct. 1988)
188. Cline, D., Presented at 5th Sporadic Meet. North Calif. Supernova Dealers Assoc., Livermore (March 1988)
189. Freese, K., *Phys. Lett.* 167B: 295 (1986)
190. Fresse, K., Frieman, J., Gould, A., In preparation (1988)
191. Gunn, J., et al., *Astrophys. J.* 233: 1015 (1978)
192. Stecker, F. W., *Astrophys. J.* 233: 1032 (1978)
193. Turner, M., *Phys. Rev. D*34: 1921 (1986)
194. Ellis, J., et al., Preprint in preparation (1988)
195. Srednicki, M., Thiesen, S., Silk, J., *Phys. Rev. Lett.* 56: 263 (1986)
196. Rudaz, S., *Phys. Rev. Lett.* 56: 2128 (1986)
197. Fichtel, C. E., et al., *Astrophys. J.* 217: L9 (1977)
198. Bloemen, J. B. G. M., et al., *Astron. Astrophys.* 154: 25 (1986)
199. Hillier, R., *Gamma Ray Astronomy*. Oxford: Clarendon (1984)
200. Ramana Murthy, P., Wolfendale, A., *Gamma-Ray Astronomy*. Cambridge Univ. Press (1986)
- 200a. Dermer, C. D., *Astron. Astrophys.* 157: 223 (1986)
201. Silk, J., Bloemen, H., *Astrophys. J. Lett.* 313: L47 (1987)
202. Blitz, L., et al., *Astron. Astrophys.* 143: 267 (1985)
203. Stecker, F. W., *Phys. Lett.* 201B: 529 (1988)
204. Ipsier, J., Sikivie, P., *Phys. Rev. D*35: 3695 (1987)
205. Hughes, et al., *NASA Tech. Memo. 80590*, Washington, DC (1979)
206. Sadoulet, B., High Energy All Sky Imager (HEASI) Explorer. *Proposal UCBSL 1304/86*. Submitted to NASA (1986)
207. Stecker, F. W., Rudaz, S., Walsh, T. F., *Phys. Rev. Lett.* 55: 2622 (1985)
208. Hagelin, J. S., Kane, G. L., *Nucl. Phys.* B263: 399 (1986)
209. Ginzburg, V., Ptuskin, V., *Rev. Mod. Phys.* 48: 161 (1976)
210. Perko, J., *Astron. Astrophys.* 184: 119 (1987)
211. Golden, R. L., et al., *Phys. Rev. Lett.* 43: 1196 (1979)
212. Buffington, A., et al., *Astrophys. J.* 248: 1179 (1981)
213. Ahlen, S. P., et al., *Phys. Rev. Lett.* Submitted (1988)
214. Tytka, A. J., Eichler, D., *Univ. Maryland Preprint* (1988)
215. Kim, J. E., *Phys. Rep.* 150: 1 (1987)
216. Cheng, H.-Y., *Phys. Rep.* 158: 1 (1988)
217. Sikivie, P., In *Particles and the Universe*, ed. G. Lazarides, Q. Shafi. Netherlands: Elsevier (1986), pp. 201-14

218. Peccei, R., Quinn, H., *Phys. Rev. Lett.* 38: 140 (1977)
219. Weinberg, S., *Phys. Rev. Lett.* 40: 223 (1978)
220. Wilczek, F., *Phys. Rev. Lett.* 40: 279 (1978)
221. Dine, M., Fischler, W., Srednicki, M., *Phys. Lett.* 104B: 199 (1981)
222. Zhitnitsky, A. R., *Sov. J. Nucl. Phys.* 31: 260 (1980)
223. Kim, J. E., *Phys. Rev. Lett.* 43: 103 (1979)
224. Shifman, M. A., Vainshtein, A. I., Zakharov, V. I., *Nucl. Phys.* B166: 493 (1980)
225. Kaplan, D. B., *Nucl. Phys.* B260: 215 (1985)
226. Sikivie, P., In *The Architecture of Fundamental Interactions at Short Distances*, les Houches Summer School (1985)
227. Srednicki, M., *Nucl. Phys.* B260: 689 (1985)
228. Ipser, J., Sikivie, P., *Phys. Rev. Lett.* 50: 925 (1983)
229. Abbott, L., Sikivie, P., *Phys. Lett.* 120B: 133 (1983)
230. Dine, M., Fischler, W., *Phys. Lett.* 120B: 137 (1983)
231. Preskill, J., Wise, M., Wilczek, F., *Phys. Lett.* 120B: 127 (1983)
232. Turner, M., *Phys. Rev. D*33: 889 (1986)
233. Cheng, H.-Y., *Phys. Rev. D*36: 1649 (1987)
234. Dearborn, D. S. P., Schramm, D. N., Steigman, G., *Phys. Rev. Lett.* 56: 26 (1986)
235. Raffelt, G., *Phys. Lett.* 166B: 402 (1986)
236. Raffelt, G., *Phys. Rev. D*33: 897 (1986)
237. Dearborn, D. S. P., Raffelt, G., *Phys. Rev. D*36: 2211 (1987)
238. Avignone, F. T., et al., *Phys. Rev. D*35: 2752 (1987)
239. Dimopoulos, S., et al., *Phys. Lett.* 179B: 223 (1986)
240. Sikivie, P., *Phys. Rev. Lett.* 51: 1415 (1983), erratum 52: 695 (1984); *Phys. Rev. D*32: 2988 (1985), erratum 36: 974 (1987)
241. von Bibber, K., et al., Letter of intent to FNAL (1988)
242. Ellis, J., Olive, K., *Phys. Lett.* 193B: 525 (1987)
243. Turner, M. S., *Phys. Rev. Lett.* 60: 1797 (1988)
244. Mayle, R., et al., *FERMILAB-Pub-87/225-A* Batavia, Ill: Fermi Natl. Accel. Lab (1987)
245. DePanfilis, et al., *Phys. Rev. Lett.* 59: 839 (1987)
246. Sikivie, P., Sullivan, N., Tanner, D., Proposal and progress reports (1984-88)
247. Krauss, L., et al., *Phys. Rev. Lett.* 55: 1797 (1985)
248. Slonozewski, J. C., *Phys. Rev. D*32: 3338 (1985)
- 248a. Flynn, J., et al., Work in progress (1988)
249. DeGrand, T., Kephart, T. W., Weiler, T. J., *Phys. Rev. D*33: 910 (1986)
250. Unruh, W. G., Wald, R. M., *Phys. Rev. D*32: 831 (1985)
251. Davis, R. L., *Phys. Lett.* 180B: 225 (1986)
252. Harari, D., Sikivie, P., *Phys. Lett.* 195B: 361 (1987)
253. Lazarides, G., Panigiotakopoulos, C., Shafi, Q., *Phys. Lett.* 192B: 323 (1987)
254. Pi, S.-Y., *Phys. Rev. Lett.* 52: 1725 (1984)
255. Kofman, L. A., Linde, A. D., *Nucl. Phys.* B282: 555 (1987)
256. Linde, A. D., *Phys. Lett.* 201B: 437 (1988)
257. Sikivie, P., *Phys. Rev. Lett.* 48: 1156 (1982)
258. Kaplan, D. B., Manohar, A., *Phys. Rev. Lett.* 56: 2004 (1986)
259. Choi, K., Kim C. W., Sze, V. K., *Johns Hopkins Preprint JHU-TIPAC-8804*. Baltimore: Johns Hopkins Univ. (1988)
260. Gershtein, S. S., Zeldovich, Ya. B., *JETP Lett.* 4: 174 (1966)
261. Cowsik, R., McClelland, J., *Phys. Rev. Lett.* 29: 669 (1972)
262. Marx, G., Szalay, A. S., In *Neutrino 72 Technoform*, Budapest, 1: 123 (1972)
263. Szalay, A. S., Marx, G., *Astron. Astrophys.* 49: 437 (1976)
264. Chikashige, Y., Mohapatra, R. N., Peccei, R. D., *Phys. Rev. Lett.* 45: 1926 (1980); *Phys. Lett.* 98B: 265 (1981)
265. Gelmini, G. B., Nussinov, S., Roncadelli, M., *Nucl. Phys.* B209: 157 (1982)
266. Langacker, P., Segrè, G., Soni, S., *Phys. Rev. D*26: 3425 (1982)
267. Freese, K., Kolb, E. W., Turner, M. S., *Phys. Rev. D*27: 1689 (1983)
268. Lyubimov, V. A., et al., *Phys. Lett.* 94B: 266 (1980); Boris, S. D., et al., *Phys. Rev. Lett.* 58: 2019-22 (1987)
269. Boehm, F., Vogel, P., *Ann. Rev. Nucl. Part. Sci.* 34: 125 (1984)
270. Boehm, F., Vogel, P., *Physics of Massive Neutrinos*. Cambridge Univ. Press (1987)
271. Kolb, E. W., Stebbins, A. J., Turner, M. S., *Phys. Rev. D*35: 3598 (1987)
272. Burrows, A., *Astrophys. J. Lett.* 328: L51 (1988)
273. Spergel, D. N., Bahcall, J. N., *Phys. Lett.* 200B: 366 (1988)

274. Schramm, D. N., *Comments Nucl. Part. Phys.* 17: 239 (1987)
275. Abbott, L. F., De Rujula, A., Walker, T. P., *Nucl. Phys.* B299: 734 (1988)
276. Aardsma, G., et al. (Sudbury collaboration), *Phys. Lett.* 194B: 321–25 (1987)
277. Bisnovatyi-Kogan, G. S., Novikov, I. D., *Sov. Astron.* 24: 516 (1980)
278. Bond, J. R., Efstathiou, G., Silk, J., *Phys. Rev. Lett.* 45: 1980 (1980)
279. Bond, J. R., Szalay, A. S., *Astrophys. J.* 276: 443 (1983)
280. White, S. D. M., In *Inner Space/Outer Space*, ed. E. W. Kolb, et al. Univ. Chicago Press (1986), p. 228
281. Brandenberger, R., et al., *Phys. Rev. Lett.* 59: 2371 (1987)
282. Bertschinger, E., Watts, P., *Astrophys. J.* 328: 23 (1988)
283. Raffelt, G., Silk, J., *Phys. Lett.* 192B: 65 (1987)
284. Faber, S. M., Lin, D. N. C., *Astrophys. J. Lett.* 266: L17 (1983)
285. Aaronson, M., et al., See Ref. 14
286. Lin, D. N. C., Faber, S. M., *Astrophys. J. Lett.* 266: L21 (1983)
287. Tremain, S. D., Gunn, J. E., *Phys. Rev. Lett.* 42: 407 (1979)
288. Cabibbo, N., Maiani, L., *Phys. Lett.* 114B: 115 (1982)
289. Langacker, P., Leveille, J. P., Sheiman, J., *Phys. Rev.* D27: 1228 (1983)
290. Tupper, G., et al., *Phys. Rev.* D35: 394 (1987)
291. Smith, P. F., Lewin, J. D., *Astrophys. J.* 318: 738 (1987)
292. Langacker, P., In *Proc. 10th Workshop on Particles and Nuclei: Neutrino Physics*, Heidelberg, October 20–22, 1987, ed. C. Schroeder. In press (1988)
293. Müller, B., See Ref. 292
294. De Rujula, A., Glashow, S., *Phys. Rev. Lett.* 45: 942 (1980)
295. Maalampi, J., Mursala, K., Roos, M., *Phys. Rev. Lett.* 56: 1031 (1986)
296. Weiler, T., *Phys. Rev. Lett.* 49: 234 (1982); *Astron. J.* 285: 495–500 (1984)
297. McCammon, D., et al., *J. Appl. Phys.* 56(5): 1263 (1984)
298. *Proc. 2nd Eur. Workshop on Low Temp. Devices for the Detection of Low Energy Neutrinos and Dark Matter* (LAPP, Annecy, France, May 2–6, 1988), ed. L. Gonzales-Mestres, D. Perrett-Gallix. Gif-sur-Yvette: Ed. Frontières. In press (1988)
299. Luke, P. N. LBL preprint. Submitted to *J. Appl. Phys.* (1988)
300. Alessandrello, A., et al., *Phys. Lett.* B202: 64 (1988)
301. Barbieri, R., Frigeni, M., Giudice, G. F., *Univ. Pisa Preprint IFUP-TH 8/88* (1988)
302. Giudice, G. F., Roulet, E., *Int. Sch. for Adv. Studies, Trieste*, preprint (1988)

NOTE ADDED IN PROOF

There has been recent progress both in the development of cryogenic detectors and in theory.

Drukier, Gonzales-Mestres, and others (298) have proposed using superconducting granules as proportional devices instead of as threshold detectors. If these schemes are practical, they will increase the potential of this method. Luke has demonstrated (299) the possibility of measuring ionization in a crystal of germanium at 1.3 K by detecting the heat produced when electrons and holes drift in an electric field. This opens the possibility of both increasing the sensitivity of ionization detectors and measuring at the same time the phonon and ionization components. Fiorini and coworkers (300) have successfully operated calorimeters of 0.7 and 10 g, admittedly with a large noise of the order of 50 keV. This is a giant step toward the large detectors needed for DM detection.

On the theoretical side, Barbieri et al (301) have extended Griest's work (114) to include Higgs exchange in models where the DM candidate is a

supersymmetric partner. If the Higgs boson is light, the elastic cross sections may be dominated by this process. Giudice & Roulet (302) find that for $M_H \lesssim 30$ GeV the Earth becomes a stronger source of high-energy neutrinos than the Sun (see Sections 2.4.1 and 2.4.2) due to the large $\sigma_{\delta N}$ for heavy elements.